Journal of Neurotrauma

Journal of Neurotrauma: http://mc.manuscriptcentral.com/neurotrauma

Brain phospholipid precursors administered post-injury reduce tissue damage and improve neurological outcome in experimental traumatic brain injury

Journal:	*Journal of Neurotrauma*
Manuscript ID	NEU-2017-5579.R1
Manuscript Type:	Regular Manuscript
Date Submitted by the Author:	27-Mar-2018
Complete List of Authors:	Thau-Zuchman, Orli; Barts and The London School of Medicine and Dentistry Blizard Institute, Neuroscience and Trauma Gomes, Rita ; Barts and The London School of Medicine and Dentistry Blizard Institute, Neuroscience and Trauma Dyall, Simon; Bournemouth university, Royal London House, Christchurch Road, Bournemouth, BH1 3LT Davis, Meirion; Barts and The London School of Medicine and Dentistry Blizard Institute, Neuroscience and Trauma Priestley, John; Barts & The London, Blizard Institute Groenendijk, Martine; Nutricia Research BV, - Nutricia Advanced Medical Nutrition DE WILDE, Martijn; Nutricia Research BV, - Nutricia Advanced Medical Nutrition Lopez-Tremoleda, Jordi; Barts and The London School of Medicine and Dentistry Blizard Institute, Neuroscience and Trauma Michael-Titus, Adina; Barts and The London School of Medicine and Dentistry Blizard Institute, Neuroscience and Trauma
Keywords:	BEHAVIORAL ASSESSMENTS, controlled cortical impact, INFLAMMATION, TRAUMATIC BRAIN INJURY, NEUROPLASTICITY
Manuscript Keywords (Search Terms):	brain phospholipids, medical multi-nutrient, traumatic brain injury, neuroprotection, neuroplasticity, functional improvement

Brain phospholipid precursors administered post-injury reduce tissue damage and improve neurological outcome in experimental traumatic brain injury

Orli Thau-Zuchman[1], Rita N. Gomes[1], Simon C. Dyall[3], Meirion Davies[1], John V. Priestley[1], Martine Groenendijk[2], Martijn C. De Wilde[2], Jordi L. Tremoleda[1], Adina T. Michael-Titus[1]

[1]Centre for Neuroscience and Trauma, The Blizard Institute, Barts and The London School of Medicine and Dentistry, Queen Mary University of London, 4 Newark Street, Whitechapel, London, E1 2AT, UK

[2]Nutricia Research - Nutricia Advanced Medical Nutrition, Utrecht, 3584 CT, the Netherlands

[3]Bournemouth University, Royal London House, Christchurch Road, Bournemouth, BH1 3LT, UK

Full contacts information:

Orli Thau-Zuchman- Corresponding author

Centre for Neuroscience and Trauma
Blizard Institute
Queen Mary University of London
4 Newark Street
London, E1 2AT, UK
Tel: +44 (0)20 7882 2281
Email: o.thau-zuchman@qmul.ac.uk

Rita N. Gomes
Centre for Neuroscience and Trauma
Blizard Institute
Queen Mary University of London
4 Newark Street
London, E1 2AT, UK
Tel: +44 (0)20 7882 2281
Email: ritanlgomes@gmail.com

Simon C. Dyall

Bournemouth University,

Royal London House,

Christchurch Road,

Bournemouth, BH1 3LT, UK

Tel: +44 (0) 1202 961896

Email: sdyall@bournemouth.ac.uk

Meirion Davies

Centre for Neuroscience and Trauma

Blizard Institute

Queen Mary University of London

4 Newark Street

London, E1 2AT, UK

Tel: +44 (0)20 7882 7165

Email: meirion.davies@qmul.ac.uk

John V. Priestley

Centre for Neuroscience and Trauma

Blizard Institute

Queen Mary University of London

4 Newark Street

London, E1 2AT, UK

Tel: +44 (0)20 7882 2281

Email: j.v.priestley@qmul.ac.uk

Martine Groenendijk

Nutricia Research

Nutricia Advanced Medical Nutrition,

Uppsalalaan 12

Utrecht Science Park
3584 CT Utrecht, 3584 CT, the Netherlands
Tel: +31 30 209 5000
Email: martine.groenendijk@nutricia.com

Martijn C. De Wilde
Nutricia Research
Nutricia Advanced Medical Nutrition,
Uppsalalaan 12
Utrecht Science Park
3584 CT Utrecht, 3584 CT, the Netherlands
Tel: +31 30 209 5000
Email: martijn.dewilde@nutricia.com

Jordi L. Tremoleda
Centre for Neuroscience and Trauma
Blizard Institute
Queen Mary University of London
4 Newark Street
London, E1 2AT, UK
Tel: +44 (0)20 7882 2295
Email: j.lopez-tremoleda@qmul.ac.uk

Adina T. Michael-Titus
Centre for Neuroscience and Trauma
Blizard Institute
Queen Mary University of London
4 Newark Street
London, E1 2AT, UK
Tel: +44 (0)20 7882 2290
Email: a.t.michael-titus@qmul.ac.uk

Running title:

Brain phospholipid precursors improve outcome after TBI

Keywords

brain phospholipids; medical multi-nutrient; traumatic brain injury; neuroprotection; neuroplasticity; functional improvement

Abstract

Traumatic brain injury (TBI) leads to cellular loss, destabilisation of membranes, disruption of synapses and altered brain connectivity, and increased risk of neurodegenerative disease. A significant and long-lasting decrease in phospholipids (PL), essential membrane constituents, has recently been reported in plasma and brain tissue, in human and experimental TBI. We hypothesised that supporting PL synthesis post-injury could improve outcome after TBI. We tested this hypothesis using a multi-nutrient combination designed to support the biosynthesis of phospholipids and available for clinical use. The multi-nutrient Fortasyn® Connect (FC) contains polyunsaturated omega-3 fatty acids, choline, uridine, vitamins, co-factors required for PL biosynthesis, and has been shown to have significant beneficial effects in early Alzheimer's disease. Male C57BL/6 mice received a controlled cortical impact injury and then were fed a control diet or a diet enriched with FC for 70 days. FC led to a significantly improved sensorimotor outcome and cognition, reduced lesion size and oligodendrocyte loss, and it restored myelin. It reversed the loss of the synaptic protein synaptophysin and decreased levels of the axon growth inhibitor Nogo-A, thus creating a permissive environment. It decreased microglia activation and the rise in ß-amyloid precursor protein and restored the depressed neurogenesis. The effects of this medical multi-nutrient suggest that support of PL biosynthesis after TBI, a new treatment paradigm, has significant therapeutic potential in this neurological condition for which there is no satisfactory treatment. The multi-nutrient tested has been used in dementia patients, is safe and well-tolerated, which would enable rapid clinical exploration in TBI.

Introduction

Traumatic brain injury (TBI) is a leading cause of death and disability [1-3] and survivors suffer from cognitive and psychological disorders. The deficits post-TBI result from multiple neurochemical and metabolic events, [4] leading to neuronal loss, dendritic, axonal and synaptic changes, [5] and white matter abnormalities. [6-8] TBI increases the risk of neurodegenerative diseases such as Alzheimer's disease (AD) [9] and Parkinson's disease. [10]

Experimental and human TBI observations report significant synaptic alterations. [11-15] Brain connectivity is disrupted in TBI patients and this is related to cognitive dysfunction. [16, 17] Phospholipids (PL) are key to the structure of membranes, and TBI triggers significant changes in PL. A decrease in brain PL, following phospholipase activation, was reported in rat controlled cortical impact injury (CCI) 4 days post-TBI and was still detected at 35 days. [18] Homayoun and colleagues reported changes in free fatty acids, a consequence of PL degradation, as early as 30 min post-CCI. [19] Changes in PL have been reported in CSF and brain tissue of TBI patients, and in mice post-CCI. [20, 21] Plasma lipidomics shows lower levels of PL in chronic TBI in humans. [22] This raises the question whether PL breakdown could become a treatment target in TBI.

Membranes contain high levels of PL; [23, 24] the "Kennedy pathway", a series of biochemical reactions which represent the main mechanism by which mammalian cells synthesize PL such as phosphatidylcholine and phosphatidylethanolamine, uses precursors such as uridine, choline and polyunsaturated fatty acids (PUFA) such as the omega-3 PUFA docosahexaenoic acid (DHA) [25, 26]. Lower levels of PUFA, and a decreased ratio DHA: arachidonic acid (AA) in PL were detected in brain and plasma in mice post-CCI. [21] Low plasma choline was reported in TBI patients. [27] This suggests that TBI creates a need for sustained support of PL biosynthesis, which could be addressed by providing precursors.

Studies on PL biosynthesis [28, 29] have led to the development of a medical multi-nutrient, Fortasyn® Connect (FC), designed to support PL formation. FC contains DHA and also the omega-3 PUFA eicosapentaenoic acid (EPA), and uridine monophosphate (UMP), choline, folic acid, vitamins B12, B6, C, and E, and selenium, required for PL biosynthesis. FC supports synaptogenesis [29-31] and improves learning and memory. [30, 32] FC protects against β-amyloid toxicity [33] and the beneficial impact of FC on memory impairment in early AD is supported by several clinical trials. [34-36] As TBI leads to a decrease in PL levels in brain and plasma, we hypothesized that FC, by providing PL precursors, could have significant beneficial effects in TBI.

The aim was to test the effect of a FC- supplemented diet in mice with CCI injury, a model which reproduces clinically relevant neurobehavioral changes, [37] and where PL changes have been documented over a long period post-injury. [21] Microglial activation, hippocampal neurodegeneration and myelin loss persist up to one year in CCI. [38] CCI studies have reported protracted increases in lesion volume [39] and impairment of spatial learning and memory. [40] We hypothesized that administration of FC post-TBI could improve neurological outcome and counter tissue loss.

Materials and Methods

Animals

Adult 10-12 week-old male C57BL/6 mice, 22-27 g (Charles River Laboratories, Harlow, UK http://www.criver.com/files/pdfs/rms/c57bl6/rm_rm_d_c57bl6n_mouse.aspx), were used, housed in groups of four in cages provided with enrichment objects, in a 12 h light/dark cycle, with diet and water ad libitum. Food intake and body weight were monitored daily. All animal procedures were carried out under a Project Licence approved by the Animal Welfare and Ethical Review Body, at

Queen Mary University of London and the UK Home Office, in accordance with the EU Directive 2010/63/EU.

Controlled cortical impact model

A controlled cortical impact (CCI) TBI model was used. [41] After 1-week acclimatisation period, mice were anaesthetized using ketamine (50 mg/Kg) and medetomidine (0.5 mg/Kg), administered intraperitoneally (i.p.). Mice were placed in a stereotaxic frame and a midline longitudinal incision was performed to expose the skull. A right lateral craniotomy was carried out using a pneumatic drill, 2.0 mm behind bregma and 2.5 mm lateral to the midline. CCI injury was induced using the following settings: a 3 mm impactor tip with a speed of 3 m/s, a depth of 2.2 mm and a dwell time of 100 ms, applied using the PCI3000 Precision Cortical Impactor™ (Hatteras Instruments, Inc., US). A control group underwent craniotomy only. After injury, the skull flap was placed back and the skin was sutured. Mice were allowed to recover in an incubator (37°C) until they were fully awake and active. Buprenorphine (0.05 mg/kg) administered subcutaneously (s.c.) was used pre-operatively for pre-emptive analgesia and post-operatively every 12 h for 3 days post-TBI.

Dietary supplementation

Following CCI, mice were randomized into two groups and fed with a control diet ('CCI-Control'; n=10) or with a Fortasyn® Connect (FC) multi-nutrient diet ('CCI-FC'; n=10) for 70 days (detailed composition in Table 1). The craniotomy group were fed with control diet (craniotomy; n=10), and there was no craniotomy-FC group, as the emphasis of the study was on the brain injury component. The choice of the dose used in this study was based on a previous study carried out in our group, in which we tested several dose levels. [42] The diets were formulated by Nutricia Research (Utrecht, The Netherlands) and manufactured by Ssniff (Soest, Germany), stored at − 20 °C to prevent lipid peroxidation, and fresh diet was given daily. Diet stability under these conditions has been

confirmed by the producers of the diet. No significant differences were seen in the daily food intake and body weight (Supplementary Fig. 1) between groups.

Experimental design and Behavioural testing

The testing at various days post-injury (dpi) is summarised in Figure 1. Sample size was calculated using power analysis (https://eda.nc3rs.org.uk/eda/) for pairwise post-hoc comparisons after ANOVA, to a statistical power of 90%, with a significance level $\alpha = 0.05$ to detect a 25% and 20% relative difference in sensorimotor behavioural scoring (mNSS), lesion size and histopathology (glial responses, cell proliferation and white matter), as experimental primary and secondary outcomes. All the behaviour (the primary study endpoint), was assessed in "blind", with the researcher unaware of the treatment, in accordance with ARRIVE guidelines.

Modified Neurological Severity Score (mNSS)

The mNSS was used to evaluate motor ability, balance and alertness, using a scoring system based on the ability to perform ten tasks that evaluate motor ability, balance and alertness (Supplementary Fig. 2). During the first week, testing was performed every other day, then once a week, until the end of experiment. A point was given for failure to perform a task. The tissue pathology correlates well with impairment scores and with the degree of brain oedema. [43, 44] The first mNSS was obtained 24 h after TBI.

Rotarod

The Rotarod test (Ugo Basile, France; 3 cm diameter) was used for the evaluation of motor coordination and balance and was carried out between day 1 and day 3 post-CCI. Prior to surgery, mice were trained on the Rotarod for three consecutive days. The first two trials were 60 s each, at a speed of 3 rpm, followed by a single trial at accelerating speed (3 to 20 rpm over 300 s, with

intervals of at least 25 min rest. The rest of the training days consisted of one trial at a constant speed of 3 rpm followed by two accelerating trials. The latency to fall from the Rotarod was recorded. The average of all accelerating phase scores was considered as the baseline (pre-injury score). Mice were tested during day 1-3 post-injury, in three trials a day, using the accelerating mode.

CatWalk

The Catwalk is a system for a quantitative automated assessment of gait. It consists of an enclosed walkway, a camera, and recording and analysis software (Noldus/ Tracksys Ltd, UK; RRID:SCR_004074). Dynamic gait parameters were analysed on day 2 post-CCI. Each mouse was placed individually in the walkway, which consists of a glass plate (100×15×0.6 cm) surrounded by two black Plexiglas walls, spaced 8 cm apart. The mouse was allowed to walk freely and traverse from one side to the other of the walkway. Two infrared beams spaced 90 cm apart were used to detect the arrival of the mouse and control the start and end of data acquisition. The recordings were carried out in a dark room. After each trial, the walkway was cleaned with 1% acetic acid for odour neutralization. Catwalk XT 7.0 software (Noldus) was used to analyse the data.

Morris Water Maze

The Morris water maze test (MWM) was used to assess memory deficits associated with spatial learning [45] between days 13-18 post-CCI. A 100 cm diameter pool filled with opaque water at 23°C was placed inside a white tent, ensuring light uniformity, with 4 visible cues hung 10 cm from the pool walls and a 11 cm diameter Plexiglas resting platform submerged 0.5 cm below the water level. Swimming performance (e.g. path, distance, speed and latency) was tracked using software (ANYmaze, Smart, Bioseb, France; RRID:SCR_014289). A learning period of 5 consecutive days (days 13-17 post-injury) and a probe trial on day 6 (day 18 post-injury) were used. During the learning period, each mouse was subjected to 4 trials a day, in the pool divided into 4 virtual

quadrants. The position of the platform was constant throughout the training session, while the starting position on each of the 4 training trials was changed. If a mouse did not find the platform within 60 s, it was guided to it. After reaching the platform, mice were allowed to stay there for 15 s. During the probe trial, mice were allowed to swim for 60 s in the absence of the platform, and the time it took to first enter the quadrant that had previously hosted the platform, was measured.

Novel Object Recognition

The novel object recognition (NOR) test was used to evaluate recognition memory on day 26 post-CCI. In the habituation phase, on days 22-25 post-injury, animals were exposed to an empty opaque box used as an open field, for 10 min. Twenty-four hours later, in a familiarization phase, each animal was given 20 min to explore two identical objects, placed in the same open field. Four hours later, in the second test phase, animals were exposed to two dissimilar objects placed in the same open field: one familiar object used in the first phase, and one novel object. In the test phase, the exploration time was 10 minutes and time spent exploring each of the objects was measured. Performance was tracked with software (ANYmaze, Smart, Bioseb, France). A recognition index (RI), i.e. the time spent investigating the novel object relative to the total object investigation, was calculated as follows: percentage time spent with novel object/time spent with novel and familiar objects. Mice that discriminate between the old and new object should have a RI above 50%. [46]

Elevated Zero Maze

An elevated zero maze test (EZM) was used to assess exploratory behaviour in an anxiety-provoking environment. Anxiety is expressed by spending more time in the enclosed quadrants. On day 45 following CCI or craniotomy, mice were individually placed in a closed quadrant, and allowed to freely explore the maze for 5 min. A camera tracked the animal, and ANYmaze software calculated the time spent in the open quadrants, the head dips (downward movement of the head

towards the floor) and stretch-attenuated postures (elongation of the body with the feet remaining in place) from the closed arms, and the total distance travelled during the test.

BrdU injections

From day 63 post-injury or craniotomy, and for 7 sequential days, animals received i.p. injections of 5-bromo-2-deoxyuridine (BrdU; 50 mg/kg, twice a day), to assess cell proliferation.

Histology and immunohistochemistry

At day 70 post-TBI, 5 animals from each group were deeply anaesthetized with sodium pentobarbital (50 mg/kg, i.p.; Sagatal, Rhone Merieux, Harlow, UK), and received a transcardiac perfusion with phosphate-buffered saline (PBS; 0.01 M, pH 7.4), followed by 4% paraformaldehyde (PFA) in phosphate buffer (0.1 M, pH 7.4, 4°C). The brains were dissected out and tissue blocks were paraffin-fixed for histology and immunohistochemistry (IHC) analyses. All tissue staining was performed between bregma - 1.28 and bregma -2.34, where the lesion was located. All the tissue analyses were carried out in "blind" with the researcher unaware of the treatment, in accordance with ARRIVE guidelines. 7 µm sections were deparaffinised and hydrated through xylene and ethanol baths. Sections were subjected to antigen retrieval (10 mM citrate buffer, pH 6.0, 30 min at 80°C) and then cooled at room temperature. The tissue was blocked with 5% normal donkey serum in 0.2% Triton X-100 in PBS for an hour, followed by three PBS washes. The following primary antibodies were used (overnight incubation): rat anti-BrdU (for cell proliferation; 1:200; Acris Antibodies GmbH Cat# SM1667PS Lot# RRID:AB_973414), rabbit anti-glial fibrillary acidic protein (GFAP) (for astrocytes; 1:800; Dako Cat# Z0334 Lot# RRID:AB_10013382), goat anti-Iba-1 (for microglia; 1:800; Wako Cat# 019-19741 Lot# RRID:AB_839504) and rabbit anti–translocator protein (TSPO) (for glial activation following CNS injury and inflammation; 1:100; Abcam Cat# ab109497 Lot# RRID:AB_10862345), mouse anti- APC (for oligodendroglia; 1:50; Millipore Cat# OP80 Lot# RRID:AB_2057371) rabbit anti-cleaved caspase-3 (Asp175) (for

apoptosis; Cell Signaling Technology Cat# 9661 also NYUIHC-314, 9661S, 9661L Lot# RRID:AB_2341188) and anti-doublecortin (DCX) (for immature neurons; 1:100 Millipore Cat# AB2253 RRID:AB_1586992). The secondary antibodies were Alexa 488 or Alexa 555 (Molecular Probes, Leiden, The Netherlands; 1:200), and Hoechst 33342 stain (Sigma, UK; 1 µg/ml PBS) was used to visualize nuclei. Slides were mounted and cover-slipped using Vectashield fluorescent mounting medium (H-1000; Vector Laboratories, Burlingame, CA). A subset of representative randomly selected sections across the whole lesion was used for Luxol Fast Blue (Sigma, UK) myelin staining.

For calculation of the lesion size, sections of 7 µm, 200 µm apart and spanning the entire rostro-caudal extent of the injured cortex were stained with haematoxylin and eosin. The lesion size was measured with ImageJ software (National Institutes of Health, Bethesda, MD, USA) and calculated using the equation: the contralateral (non-lesioned) hemisphere size minus the injured hemisphere size and divided by the contralateral hemisphere size [47]. The results are expressed as a percentage of hemispheric tissue.

Image capture analysis and processing

Four sections per animal were stained, per antibody. At least 24 fields were captured peri-lesionally (immediate area around the lesion, except for DCX, which was used to assess the differences in the contralateral hippocampus). Images were viewed at ×40 and photographed using a Zeiss Axioskop 2 microscope with a Hamamatsu camera (C4742-95). All image capture and quantification were performed blinded. Analyses were done using the ImageJ program and a dedicated script (JVP AutoColourCellCountsRev). The fluorescent signals under different excitation lasers were selected by thresholding and then superimposed on nuclei, for co-localization. A Zeiss LSM 710 confocal microscope was used for further characterization (ZENlite software; Zeiss, Cambridge, UK). Figures were prepared using Illustrator software (Adobe Illustrator CS6, RRID:SCR_014198). For

quantification of microglia morphology, we measured cell size with ImageJ (ImageJ 1.50i, National Institutes of Health, Bethesda, Maryland), for a minimum of 20 cells per animal, and five animals per group.

Western blot analysis

Tissue from five animals from each group (CCI or craniotomy) was used. At day 70 post-TBI, animals from each group were deeply anaesthetized with sodium pentobarbital (50 mg/kg, i.p.; Sagatal, Rhone Merieux, Harlow, UK), and they were decapitated. Brains were removed and a cube of the right hemisphere around the lesion was dissected using a brain matrix. Tissue was snap frozen and stored at -80◦C. Samples were prepared in RIPA lysis buffer (Sigma-Aldrich) complete with Protease Inhibitor Cocktail (Sigma-Aldrich) and sonicated, then centrifuged (10,000 g, 10 min, 4°C) and the supernatant was taken. Protein concentrations were determined using the Bradford assay. Equal amounts of protein (50 µg) were mixed with NuPAGE® LDS sample buffer (Thermo Fisher Scientific) and dithiothreitol (DTT) and boiled (95°C, 10 min), then separated using Mini-Protean TGX Gels, 10% (Biorad, UK) and electro-transferred onto polyvinylidene difluoride membranes (Biotrace). Membranes were blocked in 5% non-fat dry milk in Tris-buffered saline (pH 7.4), with 0.1% Tween-20 (Tris-buffered saline–Tween) for 1 h at room temperature. The primary antibodies used were: mouse anti-MBP (1:1,000; myelin marker, Abcam Cat# ab62631 Lot# RRID:AB_956157), mouse anti β-APP (1:500; amyloid peptide marker, Abcam Cat# ab11132 Lot# RRID:AB_297770), rabbit anti-Nogo-A (1:500; myelin-derived neurite growth inhibitor, Abcam Cat# ab62024 Lot# RRID:AB_956171), mouse anti-PSD-95 (1:500; post-synaptic density protein, Merck Millipore Cat# MAB1596 Lot# RRID:AB_2092365) and rabbit anti-synaptophysin (1:1000; presynaptic protein, Cell Signaling Technology Cat# 5461S Lot# RRID:AB_10698743), all diluted in 5% bovine serum albumin solution, and membranes were incubated overnight at 4◦C. The primary antibody was removed and the blots were washed in Tris-buffered saline–Tween and incubated (1 h, room temperature) in horseradish peroxidase-conjugated secondary antibodies

(1:10,000; Jackson ImmunoResearch Labs Cat# 323-005-021 Lot# RRID:AB_2314648). Reactive proteins were visualized using enhanced chemiluminescence (VWR International). Optical density was determined using ImageJ software (National Institutes of Health, RRID:SCR_003070). All membranes were also incubated with a mouse polyclonal antibody for β-actin (1:4,000; Sigma-Aldrich Cat# A5316 Lot# RRID:AB_476743). Protein level was expressed as relative optical density, i.e. the optical density of the band revealed by the primary antibody, divided by the optical density of β-actin in the same lane.

Phospholipid fatty acid analysis

Phospholipid (PL) fatty acid content of plasma was determined as described. [48] Lipids were extracted using the method of Folch and co-workers [49] with 0.01% w/v 2,6-di-tert-butyl-p-cresol (butylated hydroxytoluene, BHT) added as antioxidant. Total PL were isolated by thin layer chromatography and the PL fatty acid composition was measured after transesterification with 14% boron trifluoride in methanol. Fatty acids were identified by gas chromatography with flame ionisation detector (Agilent 7820A, Agilent Technologies) using an Omegawax® capillary column (15 m × 0.10 mm × 0.10 μm). The identity was confirmed by retention times compared to standards and quantification was performed on peak areas with ChemStation software (Agilent Technologies). Corrections were made for variations in the detector response and values of the fatty acids were normalised to 100% and expressed as wt %.

PL content of the cerebellum was measured as previously. [50] Neutral and acidic PL were isolated from a total lipid extract by solid phase extraction using Isolute® bonded phase aminopropyl columns (Kinesis, Beds, U.K.). The neutral PL extract was separated into phosphatidylcholine (PC) and phosphatidylethanolamine (PE) by thin-layer chromatography and the phosphate content measured. The results were normalised to 100 mg wet tissue weight.

Data analysis

Statistical analyses were done out using GraphPad Prism 5 (Graphpad Prism, RRID:SCR_002798). Data was expressed as mean ± SEM. Groups were compared using one- or two-way ANOVA followed by different post-hoc tests for multiple comparisons, and significance level set at $P<0.05$.

Results

FC supplementation improves sensorimotor impairment after TBI

TBI survivors experience sensorimotor impairment, including paresis, postural imbalance, gait disturbance, [51] and disrupted startle response. [52] TBI leads to bradykinesia, abnormal sway and impaired reaction time. [53, 54] Early balance impairment is a predictor of worse outcome post-TBI. Sensorimotor problems improve over time, although some deficits may persist beyond the first 1-2 years post-trauma. [51]

Sensorimotor impairment was assessed with mNSS, Rotarod and gait analysis. All groups showed a decrease in TBI-induced impairment over 70 days, but a significant improvement was observed in CCI FC-treated animals as early as the 3rd day post-trauma, compared to the CCI-control diet group. This difference in mNSS was maintained until the end (Two way ANOVA; $p < 0.0001$, $F_{(2,27)} = 320.8$; Fig. 2a). The craniotomy control animals showed only a transient impairment. The tasks where impairment was the most prolonged were the tasks related to balance, i.e. the round and triangular stick balance tasks and the 1 cm-beam walk task.

The Rotarod results in the 3 days post-injury (dpi) revealed better performance in FC-treated animals (One way ANOVA; $p < 0.0001$, $F_{(2,26)} = 42.31$;Fig. 2b). The latency to fall off the Rotarod was significantly higher in the FC-supplemented animals, compared to control CCI animals. The craniotomy-control group showed minimal coordination and balance impairment.

Gait analysis at 2 dpi using the Catwalk system revealed impaired locomotion in CCI-control diet animals. A long print length reflects foot dragging and less control of the foot. We also noticed after injury a smaller print width and a smaller print area within the left hind paw (LH) in the control diet group, which indicate a poor control of the paw placement. The FC-treated group showed a decrease in print length for the LH compared to the control diet group. We also assessed the stand index (SI) which measures the speed at which the paw loses contact with the glass plate. The SI was higher in CCI-control diet animals compared with the other groups, emphasising a poor support of the LH during locomotion. The step cycle, which runs from the initial contact to the following contact of the same paw, was longer in the CCI-control diet group. We also noticed a slower body speed in this group compared to CCI-FC and craniotomy-control animals. These latter two parameters may reflect a motor 'clumsiness' that is a consequence of the impaired relationship between the placement of paws within a step. The measurements indicated that TBI reduced interlimb coordination and the FC diet led to partial improvement. (Supplementary Fig. 3).

FC improves spatial memory deficits in the MWM and reduces novel object recognition impairment after TBI

TBI leads to deficits in cognition, e.g. memory, attention and information-processing speed, which are TBI severity-dependent. The temporal lobes are vulnerable in TBI, in part because of their location in the skull. The hippocampus plays a key role in memory processing, recognition, acquisition, and storage of the contextual details and temporal order of stimuli; hippocampal atrophy is related to injury severity. [55, 56] . Spatial memory was assessed using the Morris water maze (MWM), a test used to detect impairments in hippocampal-dependent learning and memory. [57] CCI led to a disruption of the task acquisition and the FC –supplemented animals did not show significant differences compared to the injured animals fed the control diet (Supplementary Fig. 4). The probe trial revealed a major impairment post-CCI (One way ANOVA; $p = 0.0005$, $F_{(2,27)} = 10.17$; Fig. 2c), which was reversed by the FC-supplemented diet.

The novel object recognition (NOR) task is another widely used model for the investigation of memory. Observations in primates and rodents have shown the importance of the parahippocampal regions of the temporal lobe (perirhinal, entorhinal and inferior temporal cortices) for visual object recognition memory [58].

In the NOR, craniotomy -control mice spent the highest proportion of time with the novel object (One way ANOVA; $p = 0.003$, $F_{(3,36)} = 5.596$; Fig. 2d). CCI resulted in a significant reduction in the recognition index (RI), and this reduction was partly reversed by FC.

FC reverses the disrupted behaviour in the elevated zero maze after TBI

TBI survivors frequently present with a delayed emergence of increased anxiety, agitation and disinhibition, and aggressive behavior. [59] These changes in personality disrupt relationships and hinder rehabilitation. Anxiolytic and anxiogenic factors can be tested using the elevated plus maze, during which the animals display a preference for dark spaces. In a CCI study, it was shown that at 21 days post-injury, mice display a reduced anxiety. [60]

We tested the impact of CCI in the elevated-zero maze (EZM), a modification of the elevated plus maze that eliminates the central region of the maze, thus focusing the analysis on the behaviour in the closed and open spaces. [61] CCI-injured mice fed with control diet showed a reduced level of anxiety compared to control-craniotomy mice, resulting in an increased exploration time in the open areas. This correlated with a lower number of head dips from the closed arms and a higher distance travelled compared with CCI-FC and craniotomy-control mice. Therefore, TBI led to a disinhibition of mice, and in CCI mice receiving FC, the multi-nutrient reduced this behavioural disinhibition (One way ANOVA; Total distance $p = 0.0068$, $F_{(2,12)} = 7.799$; Head dips $p = 0.0001$, $F_{(2,12)} = 21.92$; Time spent in open arms $p = 0.0004$, $F_{(2,12)} = 16.52$; Fig. 2e).

FC supplemented animals show a significant reduction in lesion size

TBI is associated with a reduction in brain volume, which continues for years after the injury. [62] Analysis of the lesion size showed that at 70 dpi there was a significant loss of tissue, with almost total loss of ipsilateral hippocampus. FC supplementation significantly decreased lesion size (One way ANOVA; $p < 0.0001$, $F_{(2,33)} = 382.5$; Fig. 3a, b). There was no difference in neuronal numbers (NeuN-positive cells) perilesionally, between the three groups (not shown).

FC supplementation leads to a decrease in microglia activation and alters the astrocyte response post-injury

Microglia are brain immune cells derived from the yolk sac, [63] with phagocytic and antigen-presenting properties, [64] which exert constant brain surveillance. [65] Their activation is a hallmark of TBI [66] and is reflected in morphological changes, from a quiescent ramified morphology [67] to an amoeboid aspect. [68] TBI leads to microglial activation, which can be detected in humans years after injury. [69] This long-lasting response has also been described in mouse CCI. [38] One of the markers of microglia activated after TBI is the translocator protein (TSPO), located in the mitochondrial membrane. [70] PET imaging has shown an increase in TSPO post-TBI in humans [71] and in rat CCI. [72] We investigated the microglial response with the Iba-1 and TSPO markers. The percentage of Iba-1 positive cells around the lesion was higher in the CCI-control diet group compared to FC-CCI and craniotomy groups. (One way ANOVA; $p = 0.0032$, $F_{(2,11)} = 10.1$; Fig. 4a, b). FC led to an overall decrease in TSPO- positive cells compared to control diet-treated CCI animals (One way ANOVA; $p < 0.0001$, $F_{(2,11)} = 273.7$; Fig. 4a,c). The staining for TSPO and Iba-1 showed a significantly lower number of double-stained cells in the FC-supplemented group compared to the CCI group on control diet (One way ANOVA; $p < 0.0001$, $F_{(2,11)} = 77.97$; Fig. 4a,d). Notable differences in glia morphology were seen between the CCI-control diet group (predominantly amoeboid), the CCI-FC diet group (less amoeboid) and craniotomy-control group (predominantly ramified). Therefore, we conducted an additional cell-size analysis to underline morphological

differences in the two CCI groups. Microglial cell size in the CCI-control diet group was significantly larger compared with the CCI-FC group (Mann Whitney test p= 0.0079; Fig. 4e).

Astrocytes are part of the brain macroglia and are activated following TBI; [73, 74] this is due to the traumatic impact per se, as well as the ischaemia, disruption of the blood-brain barrier, inflammation and other metabolic changes post-injury. The astrogliotic reaction is reflected in both proliferation and cell hypertrophy. [75, 76] These processes can be followed using quantification of intermediate filament proteins and by labelling the newly formed astrocytes. *In vivo* imaging shows the heterogeneity of the astrocytic response after injury in mice, i.e. the existence of proliferative and non-proliferative subpopulations. [75] After injury, astrocytes can exert both damaging and protective effects. Some astrocytes are lost in the first days post-injury, [77] whereas later on these cells are involved in the formation of the perilesion scar. [78] Ablation of proliferative astrocytes post-CCI in mice leads to a worse outcome, suggesting that the astrocytic response and the scar limit the injury impact. [79] During remodelling post-TBI, astrocytes may help maintain neuronal excitability. [80]

CCI led to an increase in astrocyte staining in the perilesional area vs. craniotomy-only animals, without any differences between the control and FC-supplemented diet (One way ANOVA; $p <$ 0.0001, $F_{(2,12)} = 40.37$;Fig. 5a,c). The determination of the newly-formed astrocytes, i.e. cells double-labelled with BrdU and GFAP, showed an intense proliferation at 70 dpi, which was amplified by FC supplementation (One way ANOVA; $p < 0.0001$, $F_{(2,12)} = 119.4$; Fig. 5a,d).

FC supplementation modulates cell proliferation and neurogenesis after CCI

CCI leads to a robust increase in cell proliferation, which involves both glial progenitors and cells in the neurogenic niche. [81] The increase in the first hours post-injury is in the subventricular zone, whereas later on an increase in BrdU-labelled cells can be detected throughout the lesioned hemisphere, and also contralaterally. [82] TBI is also associated with changes in neurogenesis. A

decreased number of immature neurons has been reported in mouse CCI in the first week after injury, ipsilaterally and contralaterally. [83] The assessment of the proliferating cells after CCI showed a significantly higher percentage of BrdU- positive cells perilesionally compared to the craniotomy control group. The treatment with FC led to a markedly increased cell proliferation peri-lesionally (One way ANOVA; $p < 0.0001$, $F_{(2,12)} = 131.5$; Fig.5a, b), and contralaterally, in the dentate gyrus (DG) (One way ANOVA; $p = 0.0098$, $F_{(2,9)} = 8.069$; Fig. 6a, c). In the contralateral hippocampus CCI decreased the number of immature neurons (doublecortin-positive cells; DCX), to less than half the value detected in craniotomy-control animals (One way ANOVA; $p = 0.0009$, $F_{(2,6)} = 27.64$; Fig. 6b, d). Supplementation with FC restored the number of immature neurons to the level seen in craniotomy-control animals.

FC supplementation leads to protection of myelin and oligodendrocytes after TBI

Imaging and post-mortem studies show that altered white mater integrity is a major consequence of TBI. [84-86] Oligodendrocytes have a key role in the white matter repair post-trauma. [87] The demyelination response after injury in mice is already detected 3 days after injury, with evidence of remyelination by the end of the first week post-injury. [88]

Luxol Fast Blue (LFB) staining showed myelin disruption after CCI, particularly in the caudate-putamen and internal capsule. Qualitative analysis indicated preserved patterns of myelin in CCI-FC and craniotomy-control mice (Fig. 7a), whereas CCI-control diet animals showed severe disruption. Myelin-basic-protein (MBP) showed a statistically significant decrease in CCI mice fed with the control diet, with the levels fully restored after FC supplementation (One way ANOVA; $p < 0.0001$, $F_{(2,12)} = 27.81$; Fig. 7b). Injury reduced oligodendrocytes peri-lesionally. This CCI-induced reduction was not modified by the FC diet (One way ANOVA; $p = 0.00417$, $F_{(2,9)} = 4.619$; Fig. 7c). However, dual staining with APC and BrdU showed a much higher percentage of double-stained cells in the CCI-FC diet group compared with the other groups (One way ANOVA; $p =$

0.0028, $F_{(2,9)} = 12.09$; Fig 7d). Furthermore, double staining of APC with caspase-3, showed a significantly lower percentage of cells in the FC diet-CCI group compared with the CCI-control diet group (One way ANOVA; $p = 0.0009$, $F_{(2,9)} = 16.9$; Fig. 7e), suggesting an on-going higher rate of apoptosis in the untreated injured group. Overall, these findings support a protective effect of FC on white matter and a significant support of the proliferative pool of oligodendrocytes.

FC modulates changes in synaptic markers after CCI - synaptophysin and PSD-95

It has been shown that even mild experimental TBI, which is not associated with development of a lesion cavity, leads to dendritic degeneration of the apparently spared neurons in the perilesional area, and to loss of synapses, as evidenced using synaptophysin immunostaining, [89] as early as 3 days after injury. Furthermore, in the same mild CCI mouse model, altered dendritic spine density and marked dendritic beading and swelling were reported in the hippocampus. [13] More recently it was shown that 24 h after injury, the dendritic spine loss could be detected both in the ipsilateral and contralateral hemisphere. [90] Alterations are persistent, as changes in the cortical dendritic arbor have been reported at 4 months post-CCI. [91] A significant decrease in the post-synaptic marker PSD-95 has been reported after CCI, at a time when the animals displayed cognitive impairment. [92]

The CCI group on a control diet showed a significant decrease in synaptophysin. In contrast, in the CCI-FC group, the level of synaptophysin was almost the same as that found in the craniotomy-control group (One way ANOVA; $p < 0.0001$, $F_{(2,12)} = 35.5$; Fig 8a). We found a similar trend in the postsynaptic protein PSD-95, which was reduced after CCI and restored after FC supplementation – however, these changes were not statistically significant (One way ANOVA; $p = 0.4188$, $F_{(2,12)} = 0.9365$; Fig. 8b).

FC decreases the neurite outgrowth inhibitor and amyloid load

TBI leads to compensatory neuroplasticity, and a major impediment to recovery is the limited axonal regeneration. Factors such as the myelin-associated inhibitor Nogo-A are linked to limited

plasticity after injury. An increase in Nogo-A was seen within the first week after injury, after rat fluid percussion injury and mouse CCI. [93, 94]

The level of the axon growth inhibitor Nogo-A, was up-regulated by injury and significantly reduced by the FC diet (One way ANOVA; $p = 0.0002$, $F_{(2,12)} = 18.68$; Fig. 8c).

One of the burdens associated with TBI is the increased incidence of AD in TBI survivors. [95] Changes in β-APP following TBI have been reported at both early and delayed times post-injury. An increase in β-APP has been found after CCI in rats, up to 3 days after injury. [96] We found that the tissue level of β-APP in the lesioned area was significantly increased, and reduced by the FC diet (One way ANOVA; $p = 0.0163$, $F_{(2,12)} = 5.915$; Fig. 8d).

FC alters plasma phospholipid levels of AA, EPA and DHA

The fatty acid composition of plasma PL at 70 dpi showed that the FC-supplemented group had a significantly higher level of EPA and DHA, compared to the CCI-control diet and craniotomy-control. In contrast, a significantly lower level of AA was found in the CCI-FC group compared to the other two groups (Two way ANOVA; $p < 0.0001$, $F_{(2,93)} = 20.45$;Fig. 9a), therefore resulting in a higher DHA/AA ratio. No changes were seen in the other fatty acids (Supplementary Fig. 5). The ratio DHA/AA was reported to be lower at 3 months post-CCI [21] in particular in the phosphatidyl ethanolamine fraction of plasma PL, therefore our results show that the FC-based intervention could help improve the DHA/AA ratio post-injury.

FC alters the tissue levels of PC and PE

The analysis of PL composition in the cerebellum showed that PC levels decreased vs. craniotomy controls by 20% after CCI, and after FC supplementation the difference vs. craniotomy controls was reduced to 11%. PE levels decreased by 21% in the injured animals on the control diet vs. craniotomy-only, while after FC supplementation the difference was only 8% (Two way ANOVA; $p < 0.0001$, $F_{(1,26)} = 47.12$;Fig. 9b).

Discussion

In this study we show for the first time that a specialised medical multi-nutrient which provides PL precursors and which has recently been shown to reduce hippocampal atrophy in prodromal AD[97], induces a significant neurological improvement and reduces the impact of injury when administered post-TBI. The intervention with FC in a murine injury model markedly improved outcome and reduced tissue loss.

FC improved gait, balance and motor coordination, spatial and recognition memory, and it corrected behavioural disinhibition. The wide range of improvements throughout the period post-injury were seen in parallel with beneficial effects on tissue.

Focal contusion TBI, such as that induced in CCI, ultimately creates cavitation at the injury epicentre. The tissue loss is linked to the sensorimotor and cognitive deficits. [98] The lesion was decreased after PL precursor supplementation, and lesion reduction could be correlated with improved outcome. [99] The multi-nutrient also modified neuroinflammation. Microglia play a major role in the inflammatory response post-TBI. [100] FC reduced the activated microglia peri-lesionally. Activated microglia express the cholesterol transporter protein TSPO, and CCI led to an increase in TSPO. Other studies have reported an increase in TSPO in models of TBI [101] [72] and TBI patients. [71] FC supplementation significantly reduced TSPO expression at 70 days post-CCI.

Microglial activation may relate to white matter disruption. [102] The co-localisation of MBP immunoreactivity with microglia after TBI suggests that myelin fragments could provide a persistent trigger for inflammation, by stimulating microglial activation. [103] The increased activated microglia after TBI also correlate with elevated tissue levels of β-amyloid (Aβ). [104] The reduction in activated microglia around the lesion, after FC, may have contributed to axonal protection by lessening the accumulation of Aβ. This accumulation occurs in damaged axons after TBI, and axonal injury can be detected using labelling for the amyloid precursor protein (β-APP). [16, 74, 105, 106]

Our data show an increased expression of β-APP in injured tissue, as reported previously [107, 108] and supplementation with FC partially reversed this.

Astrocytes have a pivotal role after TBI and undergo reactive astrogliosis. [80] Astrocytes control leukocyte infiltration, blood-brain barrier repair and neuronal degenerative processes post-TBI, act as buffers for neurotransmitter excess and modulate neurovascular coupling. [109] Disruption of the links between astrocytes and oligodendrocytes can result in demyelination, in parallel with motor impairment. [110] Astrocytes have a role in synaptic plasticity and neural circuit reorganization, and remyelination. We show after CCI an increase in newly born astrocytes post-injury and this to a greater extent in the FC group. This may contribute to tissue repair/regeneration processes.

We also show that the PL precursor combination protects white matter and oligodendrocytes post-TBI. We found restored levels of MBP, a decreased level of oligodendrocyte death, and more newly-formed oligodendrocytes. There is a strong relationship between axon and myelin integrity - the proliferation, differentiation and maintenance of oligodendrocytes requires axon-derived signals and there is a continuous cross talk and mutual dependence. [111]

FC stimulated neurogenesis, and treatments which stimulate neurogenesis, especially in the late phase post-injury, could contribute to circuit restoration[112-115]. Functional recovery also depends on axonal regeneration and sprouting, which underlie the neuroplastic changes that accompany recovery. [116] We found that the sustained supply of FC significantly reduced Nogo-A, a myelin component which inhibits axonal growth, [117] thus showing that FC enables a supportive environment for axons. These results are in agreement with Wurtman and colleagues, who showed lower levels of Nogo-A in aged rats after supplementation with these precursors, [118] and in accord with observations on FC supplementation after spinal cord compression, [20] .

The multi-nutrient FC was developed to prevent destabilisation and loss of synapses, an early feature of AD, [119] and several studies support this mechanism of action. [36] In our study, the

presynaptic protein synaptophysin and the postsynaptic protein PSD-95 were used to assess synapse loss post-TBI. In the FC group, we saw a total reversal in the decrease in synaptophysin induced by the injury, and a similar trend was seen for PSD-95.

Taken together, the data show pleiotropic beneficial effects of supplementation with PL precursors after TBI. The functional improvement using neurological endpoints is correlated with improved tissue aspect, ipsilaterally and also in the contralateral hemisphere (which has an important role in recovery after injury). [116]

PC and PE levels were reduced after CCI even at a distance from the injury site, as reported previously,[18, 19] and FC reduced these losses.

The multi-nutrient used in this study provides precursors for the formation of phospholipids (PL)[31], and this novel therapeutic strategy addresses mechanistically the chronic decrease in PL detected after TBI in humans. [22] This consequence of injury is persistent, i.e. detectable at 24 months post-trauma, in an impact brain injury model in mice[120], suggesting that it is a fundamental process of destabilisation of membranes, seen across species. Stocchetti et al. have proposed a list of key requirements for treatments for TBI tested pre-clinically, in order to increase the chances of successful clinical translation. [121] The PL precursor combination tested here satisfies several requirements: *i)* the relevance of the targeted mechanism (i.e. there is a reported sustained decrease of 25-35% in several PL classes post-injury after TBI, *ii)* the treatment tested can increase brain PL levels after 4-6 weeks of supplementation (as shown by Cansev et al in aged rats[122] and our data here), and *iii)* the PL precursor preparation has been previously shown to restore brain connectivity and reduce hippocampal loss in patients, in early AD, as supported by clinical trials with FC. [34, 123, 124]

TBI triggers many injury mechanisms, which should be addressed using multimodal treatments. [125] Specialised nutrient interventions have the benefit of addressing multimodal mechanisms, [126] and

FC is a unique concept focused on the support of membrane integrity through provision of precursors required for PL formation. Injury in the nervous system triggers an extensive reorganisation of circuits ipsilaterally and in the opposite hemisphere, and it could be hypothesised that FC might provide support for such restorative processes. [116, 127-129]

Our results show that the novel concept of providing PL precursors post-injury could have therapeutic potential in TBI. Future studies should explore in detail in several TBI models the time window for administration and the optimum duration of intervention, in order to increase the likelihood of translational success.

Funding and Acknowledgments

OTZ, MD and JLT were supported by the Centre for Trauma Sciences, Barts Charity grant. MG and MCdW are employees of Nutricia Research. AMT is a scientific consultant for Nutricia Research.

We thank J. Priestley for the ImageJ script, P. Pallier for contribution to behavioural testing, F. de Giorgio for advice with blotting, A. Volianskis for support with figures. AMT, OTZ and JLT designed the experiments. OTZ carried out in vivo and ex vivo work and analysed the data. AMT, OTZ and JLT wrote the manuscript. JLT carried out the surgery. MD and OTZ helped with surgery. ARG contributed to immunohistochemistry analysis. SCD carried out lipid analysis.

Author Disclosure statement

The authors declare no competing financial interests.

References

1. Roebuck-Spencer, T. and Cernich, A. (2014). Epidemiology and Societal Impact of Traumatic Brain Injury. In: *Handbook on the Neuropsychology of Traumatic Brain Injury*. Sherer, M., Sander, M.A. (eds). Springer New York: New York, NY, pps. 3-23.

2. Maas, A.I., Stocchetti, N. and Bullock, R. (2008). Moderate and severe traumatic brain injury in adults. Lancet Neurol 7, 728-741.

3. Rutland-Brown, W., Langlois, J.A., Thomas, K.E. and Xi, Y.L. (2006). Incidence of traumatic brain injury in the United States, 2003. J Head Trauma Rehabil 21, 544-548.

4. Balu, R. (2014). Inflammation and immune system activation after traumatic brain injury. Curr Neurol Neurosci Rep 14, 484.

5. Johnson, V.E., Stewart, W. and Smith, D.H. (2013). Axonal pathology in traumatic brain injury. Experimental Neurology 246, 35-43.

6. Bramlett, H.M. and Dietrich, W.D. (2002). Quantitative structural changes in white and gray matter 1 year following traumatic brain injury in rats. Acta Neuropathol 103, 607-614.

7. Mayer, A.R., Ling, J., Mannell, M.V., Gasparovic, C., Phillips, J.P., Doezema, D., Reichard, R. and Yeo, R.A. (2010). A prospective diffusion tensor imaging study in mild traumatic brain injury. Neurology 74, 643-650.

8. Kinnunen, K.M., Greenwood, R., Powell, J.H., Leech, R., Hawkins, P.C., Bonnelle, V., Patel, M.C., Counsell, S.J. and Sharp, D.J. (2011). White matter damage and cognitive impairment after traumatic brain injury. Brain 134, 449-463.

9. Sivanandam, T.M. and Thakur, M.K. (2012). Traumatic brain injury: a risk factor for Alzheimer's disease. Neurosci Biobehav Rev 36, 1376-1381.

10. Gardner, R.C., Burke, J.F., Nettiksimmons, J., Goldman, S., Tanner, C.M. and Yaffe, K. (2015). Traumatic brain injury in later life increases risk for Parkinson disease. Ann Neurol 77, 987-995.

11. Lyeth, B.G., Jenkins, L.W., Hamm, R.J., Dixon, C.E., Phillips, L.L., Clifton, G.L., Young, H.F. and Hayes, R.L. (1990). Prolonged memory impairment in the absence of hippocampal cell death following traumatic brain injury in the rat. Brain Res 526, 249-258.

12. Scheff, S.W., Price, D.A., Hicks, R.R., Baldwin, S.A., Robinson, S. and Brackney, C. (2005). Synaptogenesis in the hippocampal CA1 field following traumatic brain injury. J Neurotrauma 22, 719-732.

13. Gao, X., Deng, P., Xu, Z.C. and Chen, J. (2011). Moderate traumatic brain injury causes acute dendritic and synaptic degeneration in the hippocampal dentate gyrus. PLoS One 6, e24566.

14. Harish, G., Mahadevan, A., Pruthi, N., Sreenivasamurthy, S.K., Puttamallesh, V.N., Keshava Prasad, T.S., Shankar, S.K. and Srinivas Bharath, M.M. (2015). Characterization of traumatic brain injury in human brains reveals distinct cellular and molecular changes in contusion and pericontusion. J Neurochem 134, 156-172.

15. Merlo, L., Cimino, F., Angileri, F.F., La Torre, D., Conti, A., Cardali, S.M., Saija, A. and Germano, A. (2014). Alteration in synaptic junction proteins following traumatic brain injury. J Neurotrauma 31, 1375-1385.

16. Sharp, D.J., Scott, G. and Leech, R. (2014). Network dysfunction after traumatic brain injury. Nat Rev Neurol 10, 156-166.

17. Fagerholm, E.D., Hellyer, P.J., Scott, G., Leech, R. and Sharp, D.J. (2015). Disconnection of network hubs and cognitive impairment after traumatic brain injury. Brain 138, 1696-1709.

18. Homayoun, P., Rodriguez de Turco, E.B., Parkins, N.E., Lane, D.C., Soblosky, J., Carey, M.E. and Bazan, N.G. (1997). Delayed phospholipid degradation in rat brain after traumatic brain injury. J Neurochem 69, 199-205.

19. Homayoun, P., Parkins, N.E., Soblosky, J., Carey, M.E., Rodriguez de Turco, E.B. and Bazan, N.G. (2000). Cortical impact injury in rats promotes a rapid and sustained increase in polyunsaturated free fatty acids and diacylglycerols. Neurochem Res 25, 269-276.

20. Pasvogel, A.E., Miketova, P. and Moore, I.M. (2010). Differences in CSF phospholipid concentration by traumatic brain injury outcome. Biol Res Nurs 11, 325-331.

21. Abdullah, L., Evans, J.E., Ferguson, S., Mouzon, B., Montague, H., Reed, J., Crynen, G., Emmerich, T., Crocker, M., Pelot, R., Mullan, M. and Crawford, F. (2014). Lipidomic analyses identify injury-specific phospholipid changes 3 mo after traumatic brain injury. FASEB J 28, 5311-5321.

22. Emmerich, T., Abdullah, L., Crynen, G., Dretsch, M., Evans, J., Ait-Ghezala, G., Reed, J., Montague, H., Chaytow, H., Mathura, V., Martin, J., Pelot, R., Ferguson, S., Bishop, A., Phillips, J., Mullan, M. and Crawford, F. (2016). Plasma Lipidomic Profiling in a Military Population of Mild Traumatic Brain Injury and Post-Traumatic Stress Disorder with Apolipoprotein E varepsilon4-Dependent Effect. J Neurotrauma 33, 1331-1348.

23. Purdon, A.D., Rosenberger, T.A., Shetty, H.U. and Rapoport, S.I. (2002). Energy consumption by phospholipid metabolism in mammalian brain. Neurochem Res 27, 1641-1647.

24. Sastry, P.S. (1985). Lipids of nervous tissue: composition and metabolism. Prog Lipid Res 24, 69-176.

25. Spector, A.A. (2001). Plasma free fatty acid and lipoproteins as sources of polyunsaturated fatty acid for the brain. J Mol Neurosci 16, 159-165; discussion 215-121.

26. Moessinger, C., Klizaite, K., Steinhagen, A., Philippou-Massier, J., Shevchenko, A., Hoch, M., Ejsing, C.S. and Thiele, C. (2014). Two different pathways of phosphatidylcholine synthesis, the Kennedy Pathway and the Lands Cycle, differentially regulate cellular triacylglycerol storage. BMC Cell Biol 15, 43.

27. Ulus, I.H., Özyurt, G. and Korfali, E. (1998). Decreased Serum Choline Concentrations in Humans after Surgery, Childbirth, and Traumatic Head Injury. Neurochemical Research 23, 727-732.

28. Wurtman, R.J., Ulus, I.H., Cansev, M., Watkins, C.J., Wang, L. and Marzloff, G. (2006). Synaptic proteins and phospholipids are increased in gerbil brain by administering uridine plus docosahexaenoic acid orally. Brain Res 1088, 83-92.

29. Wurtman, R.J., Cansev, M., Sakamoto, T. and Ulus, I.H. (2009). Administration of docosahexaenoic acid, uridine and choline increases levels of synaptic membranes and dendritic spines in rodent brain. World Rev Nutr Diet 99, 71-96.

30. Kamphuis, P.J. and Wurtman, R.J. (2009). Nutrition and Alzheimer's disease: pre-clinical concepts. Eur J Neurol 16 Suppl 1, 12-18.

31. Wurtman, R.J., Cansev, M., Sakamoto, T. and Ulus, I. (2010). Nutritional modifiers of aging brain function: use of uridine and other phosphatide precursors to increase formation of brain synapses. Nutr Rev 68 Suppl 2, S88-101.

32. Wurtman, R.J., Cansev, M., Sakamoto, T. and Ulus, I.H. (2009). Use of phosphatide precursors to promote synaptogenesis. Annu Rev Nutr 29, 59-87.

33. de Wilde, M.C., Penke, B., van der Beek, E.M., Kuipers, A.A., Kamphuis, P.J. and Broersen, L.M. (2011). Neuroprotective effects of a specific multi-nutrient intervention against Abeta42-induced toxicity in rats. J Alzheimers Dis 27, 327-339.

34. Scheltens, P., Twisk, J.W., Blesa, R., Scarpini, E., von Arnim, C.A., Bongers, A., Harrison, J., Swinkels, S.H., Stam, C.J., de Waal, H., Wurtman, R.J., Wieggers, R.L., Vellas, B. and Kamphuis, P.J. (2012). Efficacy of Souvenaid in mild Alzheimer's disease: results from a randomized, controlled trial. J Alzheimers Dis 31, 225-236.

35. Scheltens, P., Kamphuis, P.J., Verhey, F.R., Olde Rikkert, M.G., Wurtman, R.J., Wilkinson, D., Twisk, J.W. and Kurz, A. (2010). Efficacy of a medical food in mild Alzheimer's disease: A randomized, controlled trial. Alzheimers Dement 6, 1-10 e11.

36. van Wijk, N., Broersen, L.M., de Wilde, M.C., Hageman, R.J., Groenendijk, M., Sijben, J.W. and Kamphuis, P.J. (2014). Targeting synaptic dysfunction in Alzheimer's disease by administering a specific nutrient combination. J Alzheimers Dis 38, 459-479.

37. Osier, N.D. and Dixon, C.E. (2016). The Controlled Cortical Impact Model: Applications, Considerations for Researchers, and Future Directions. Frontiers in Neurology 7.

38. Loane, D.J., Kumar, A., Stoica, B.A., Cabatbat, R. and Faden, A.I. (2014). Progressive neurodegeneration after experimental brain trauma: association with chronic microglial activation. J Neuropathol Exp Neurol 73, 14-29.

39. Dixon, C.E., Kochanek, P.M., Yan, H.Q., Schiding, J.K., Griffith, R.G., Baum, E., Marion, D.W. and DeKosky, S.T. (1999). One-year study of spatial memory performance, brain morphology, and cholinergic markers after moderate controlled cortical impact in rats. J Neurotrauma 16, 109-122.

40. An, C., Jiang, X., Pu, H., Hong, D., Zhang, W., Hu, X. and Gao, Y. (2016). Severity-Dependent Long-Term Spatial Learning-Memory Impairment in a Mouse Model of Traumatic Brain Injury. Transl Stroke Res.

41. Fox, G.B., Fan, L., Levasseur, R.A. and Faden, A.I. (1998). Sustained sensory/motor and cognitive deficits with neuronal apoptosis following controlled cortical impact brain injury in the mouse. J Neurotrauma 15, 599-614.

42. Pallier, P.N., Poddighe, L., Zbarsky, V., Kostusiak, M., Choudhury, R., Hart, T., Burguillos, M.A., Musbahi, O., Groenendijk, M., Sijben, J.W., deWilde, M.C., Quartu, M., Priestley, J.V. and Michael-Titus, A.T. (2015). A nutrient combination designed to enhance synapse formation and function improves outcome in experimental spinal cord injury. Neurobiol Dis 82, 504-515.

43. Beni-Adani, L., Gozes, I., Cohen, Y., Assaf, Y., Steingart, R.A., Brenneman, D.E., Eizenberg, O., Trembolver, V. and Shohami, E. (2001). A peptide derived from activity-dependent

neuroprotective protein (ADNP) ameliorates injury response in closed head injury in mice. J Pharmacol Exp Ther 296, 57-63.

44. Shapira, Y., Shohami, E., Sidi, A., Soffer, D., Freeman, S. and Cotev, S. (1988). Experimental closed head injury in rats: mechanical, pathophysiologic, and neurologic properties. Crit Care Med 16, 258-265.

45. Bourourou, M., Heurteaux, C. and Blondeau, N. (2016). Alpha-linolenic acid given as enteral or parenteral nutritional intervention against sensorimotor and cognitive deficits in a mouse model of ischemic stroke. Neuropharmacology 108, 60-72.

46. Gaskin, S., Tardif, M., Cole, E., Piterkin, P., Kayello, L. and Mumby, D.G. (2010). Object familiarization and novel-object preference in rats. Behavioural Processes 83, 61-71.

47. Swanson, R.A., Morton, M.T., Tsao-Wu, G., Savalos, R.A., Davidson, C. and Sharp, F.R. (1990). A semiautomated method for measuring brain infarct volume. J Cereb Blood Flow Metab 10, 290-293.

48. Dyall, S.C., Mandhair, H.K., Fincham, R.E., Kerr, D.M., Roche, M. and Molina-Holgado, F. (2016). Distinctive effects of eicosapentaenoic and docosahexaenoic acids in regulating neural stem cell fate are mediated via endocannabinoid signalling pathways. Neuropharmacology 107, 387-395.

49. Folch, J., Lees, M. and Sloane Stanley, G.H. (1957). A simple method for the isolation and purification of total lipides from animal tissues. J Biol Chem 226, 497-509.

50. Dyall, S.C., Michael, G.J., Whelpton, R., Scott, A.G. and Michael-Titus, A.T. (2007). Dietary enrichment with omega-3 polyunsaturated fatty acids reverses age-related decreases in the GluR2 and NR2B glutamate receptor subunits in rat forebrain. Neurobiol Aging 28, 424-439.

51. Walker, W.C. and Pickett, T.C. (2007). Motor impairment after severe traumatic brain injury: A longitudinal multicenter study. J Rehabil Res Dev 44, 975-982.

52. Saunders, J.C., McDonald, S. and Richardson, R. (2006). Loss of emotional experience after traumatic brain injury: findings with the startle probe procedure. Neuropsychology 20, 224-231.

53. Lehmann, J.F., Boswell, S., Price, R., Burleigh, A., deLateur, B.J., Jaffe, K.M. and Hertling, D. (1990). Quantitative evaluation of sway as an indicator of functional balance in post-traumatic brain injury. Arch Phys Med Rehabil 71, 955-962.

54. Gray, C., Cantagallo, A., Della Sala, S. and Basaglia, N. (1998). Bradykinesia and bradyphrenia revisited: patterns of subclinical deficit in motor speed and cognitive functioning in head-injured patients with good recovery. Brain Inj 12, 429-441.

55. Ariza, M., Serra-Grabulosa, J.M., Junque, C., Ramirez, B., Mataro, M., Poca, A., Bargallo, N. and Sahuquillo, J. (2006). Hippocampal head atrophy after traumatic brain injury. Neuropsychologia 44, 1956-1961.

56. Levine, B., Kovacevic, N., Nica, E.I., Cheung, G., Gao, F., Schwartz, M.L. and Black, S.E. (2008). The Toronto traumatic brain injury study: injury severity and quantified MRI. Neurology 70, 771-778.

57. Smith, D.H., Uryu, K., Saatman, K.E., Trojanowski, J.Q. and McIntosh, T.K. (2003). Protein accumulation in traumatic brain injury. Neuromolecular Med 4, 59-72.

58. Hammond, R.S., Tull, L.E. and Stackman, R.W. (2004). On the delay-dependent involvement of the hippocampus in object recognition memory. Neurobiol Learn Mem 82, 26-34.

59. Kim, E. (2002). Agitation, aggression, and disinhibition syndromes after traumatic brain injury. NeuroRehabilitation 17, 297-310.

60. Washington, P.M., Forcelli, P.A., Wilkins, T., Zapple, D.N., Parsadanian, M. and Burns, M.P. (2012). The effect of injury severity on behavior: a phenotypic study of cognitive and emotional deficits after mild, moderate, and severe controlled cortical impact injury in mice. J Neurotrauma 29, 2283-2296.

61. Kulkarni, S.K., Singh, K. and Bishnoi, M. (2007). Elevated zero maze: a paradigm to evaluate antianxiety effects of drugs. Methods Find Exp Clin Pharmacol 29, 343-348.

62. Farbota, K.D., Sodhi, A., Bendlin, B.B., McLaren, D.G., Xu, G., Rowley, H.A. and Johnson, S.C. (2012). Longitudinal volumetric changes following traumatic brain injury: a tensor-based morphometry study. J Int Neuropsychol Soc 18, 1006-1018.

63. Ginhoux, F., Greter, M., Leboeuf, M., Nandi, S., See, P., Gokhan, S., Mehler, M.F., Conway, S.J., Ng, L.G., Stanley, E.R., Samokhvalov, I.M. and Merad, M. (2010). Fate mapping analysis reveals that adult microglia derive from primitive macrophages. Science 330, 841-845.

64. Hickey, W.F. and Kimura, H. (1988). Perivascular microglial cells of the CNS are bone marrow-derived and present antigen in vivo. Science 239, 290-292.

65. Nimmerjahn, A., Kirchhoff, F. and Helmchen, F. (2005). Resting microglial cells are highly dynamic surveillants of brain parenchyma in vivo. Science 308, 1314-1318.

66. Hernandez-Ontiveros, D.G., Tajiri, N., Acosta, S., Giunta, B., Tan, J. and Borlongan, C.V. (2013). Microglia activation as a biomarker for traumatic brain injury. Front Neurol 4, 30.

67. Glenn, J.A., Ward, S.A., Stone, C.R., Booth, P.L. and Thomas, W.E. (1992). Characterisation of ramified microglial cells: detailed morphology, morphological plasticity and proliferative capability. J Anat 180 (Pt 1), 109-118.

68. Tambuyzer, B.R., Ponsaerts, P. and Nouwen, E.J. (2009). Microglia: gatekeepers of central nervous system immunology. J Leukoc Biol 85, 352-370.

69. Johnson, V.E., Stewart, J.E., Begbie, F.D., Trojanowski, J.Q., Smith, D.H. and Stewart, W. (2013). Inflammation and white matter degeneration persist for years after a single traumatic brain injury. Brain 136, 28-42.

70. Papadopoulos, V., Baraldi, M., Guilarte, T.R., Knudsen, T.B., Lacapere, J.J., Lindemann, P., Norenberg, M.D., Nutt, D., Weizman, A., Zhang, M.R. and Gavish, M. (2006). Translocator protein (18kDa): new nomenclature for the peripheral-type benzodiazepine receptor based on its structure and molecular function. Trends Pharmacol Sci 27, 402-409.

71. Ramlackhansingh, A.F., Brooks, D.J., Greenwood, R.J., Bose, S.K., Turkheimer, F.E., Kinnunen, K.M., Gentleman, S., Heckemann, R.A., Gunanayagam, K., Gelosa, G. and Sharp, D.J. (2011). Inflammation after trauma: Microglial activation and traumatic brain injury. Ann Neurol 70, 374-383.

72. Wang, Y., Yue, X., Kiesewetter, D.O., Niu, G., Teng, G. and Chen, X. (2014). PET imaging of neuroinflammation in a rat traumatic brain injury model with radiolabeled TSPO ligand DPA-714. Eur J Nucl Med Mol Imaging 41, 1440-1449.

73. Kimelberg, H.K. and Nedergaard, M. (2010). Functions of astrocytes and their potential as therapeutic targets. Neurotherapeutics 7, 338-353.

74. Sofroniew, M.V. and Vinters, H.V. (2010). Astrocytes: biology and pathology. Acta Neuropathol 119, 7-35.

75. Bardehle, S., Kruger, M., Buggenthin, F., Schwausch, J., Ninkovic, J., Clevers, H., Snippert, H.J., Theis, F.J., Meyer-Luehmann, M., Bechmann, I., Dimou, L. and Gotz, M. (2013). Live imaging of astrocyte responses to acute injury reveals selective juxtavascular proliferation. Nat Neurosci 16, 580-586.

76. Susarla, B.T., Villapol, S., Yi, J.H., Geller, H.M. and Symes, A.J. (2014). Temporal patterns of cortical proliferation of glial cell populations after traumatic brain injury in mice. ASN Neuro 6, 159-170.

77. Hill-Felberg, S.J., McIntosh, T.K., Oliver, D.L., Raghupathi, R. and Barbarese, E. (1999). Concurrent loss and proliferation of astrocytes following lateral fluid percussion brain injury in the adult rat. J Neurosci Res 57, 271-279.

78. Silver, J. and Miller, J.H. (2004). Regeneration beyond the glial scar. Nat Rev Neurosci 5, 146-156.

79. Myer, D.J., Gurkoff, G.G., Lee, S.M., Hovda, D.A. and Sofroniew, M.V. (2006). Essential protective roles of reactive astrocytes in traumatic brain injury. Brain 129, 2761-2772.

80. Burda, J.E., Bernstein, A.M. and Sofroniew, M.V. (2016). Astrocyte roles in traumatic brain injury. Exp Neurol 275 Pt 3, 305-315.

81. Chirumamilla, S., Sun, D., Bullock, M.R. and Colello, R.J. (2002). Traumatic brain injury induced cell proliferation in the adult mammalian central nervous system. J Neurotrauma 19, 693-703.

82. Urrea, C., Castellanos, D.A., Sagen, J., Tsoulfas, P., Bramlett, H.M. and Dietrich, W.D. (2007). Widespread cellular proliferation and focal neurogenesis after traumatic brain injury in the rat. Restor Neurol Neurosci 25, 65-76.

83. Rola, R., Mizumatsu, S., Otsuka, S., Morhardt, D.R., Noble-Haeusslein, L.J., Fishman, K., Potts, M.B. and Fike, J.R. (2006). Alterations in hippocampal neurogenesis following traumatic brain injury in mice. Exp Neurol 202, 189-199.

84. Yeh, P.H., Wang, B., Oakes, T.R., French, L.M., Pan, H., Graner, J., Liu, W. and Riedy, G. (2014). Postconcussional disorder and PTSD symptoms of military-related traumatic brain injury associated with compromised neurocircuitry. Hum Brain Mapp 35, 2652-2673.

85. Bigler, E.D. and Maxwell, W.L. (2012). Neuropathology of mild traumatic brain injury: relationship to neuroimaging findings. Brain Imaging Behav 6, 108-136.

86. Yuh, E.L., Cooper, S.R., Mukherjee, P., Yue, J.K., Lingsma, H.F., Gordon, W.A., Valadka, A.B., Okonkwo, D.O., Schnyer, D.M., Vassar, M.J., Maas, A.I., Manley, G.T. and Track-Tbi, I. (2014). Diffusion tensor imaging for outcome prediction in mild traumatic brain injury: a TRACK-TBI study. J Neurotrauma 31, 1457-1477.

87. Armstrong, R.C., Mierzwa, A.J., Sullivan, G.M. and Sanchez, M.A. (2016). Myelin and oligodendrocyte lineage cells in white matter pathology and plasticity after traumatic brain injury. Neuropharmacology 110, 654-659.

88. Mierzwa, A.J., Marion, C.M., Sullivan, G.M., McDaniel, D.P. and Armstrong, R.C. (2015). Components of myelin damage and repair in the progression of white matter pathology after mild traumatic brain injury. J Neuropathol Exp Neurol 74, 218-232.

89. Gao, X. and Chen, J. (2011). Mild traumatic brain injury results in extensive neuronal degeneration in the cerebral cortex. J Neuropathol Exp Neurol 70, 183-191.

90. Winston, C.N., Chellappa, D., Wilkins, T., Barton, D.J., Washington, P.M., Loane, D.J., Zapple, D.N. and Burns, M.P. (2013). Controlled cortical impact results in an extensive loss of dendritic spines that is not mediated by injury-induced amyloid-beta accumulation. J Neurotrauma 30, 1966-1972.

91. Hoskison, M.M., Moore, A.N., Hu, B., Orsi, S., Kobori, N. and Dash, P.K. (2009). Persistent working memory dysfunction following traumatic brain injury: evidence for a time-dependent mechanism. Neuroscience 159, 483-491.

92. Wakade, C., Sukumari-Ramesh, S., Laird, M.D., Dhandapani, K.M. and Vender, J.R. (2010). Delayed reduction in hippocampal postsynaptic density protein-95 expression temporally correlates with cognitive dysfunction following controlled cortical impact in mice. J Neurosurg 113, 1195-1201.

93. Marklund, N., Fulp, C.T., Shimizu, S., Puri, R., McMillan, A., Strittmatter, S.M. and McIntosh, T.K. (2006). Selective temporal and regional alterations of Nogo-A and small proline-rich repeat protein 1A (SPRR1A) but not Nogo-66 receptor (NgR) occur following traumatic brain injury in the rat. Exp Neurol 197, 70-83.

94. Israelsson, C., Flygt, J., Astrand, E., Kiwanuka, O., Bengtsson, H. and Marklund, N. (2014). Altered expression of myelin-associated inhibitors and their receptors after traumatic brain injury in the mouse. Restor Neurol Neurosci 32, 717-731.

95. Van Den Heuvel, C., Thornton, E. and Vink, R. (2007). Traumatic brain injury and Alzheimer's disease: a review. Prog Brain Res 161, 303-316.

96. Ciallella, J.R., Ikonomovic, M.D., Paljug, W.R., Wilbur, Y.I., Dixon, C.E., Kochanek, P.M., Marion, D.W. and DeKosky, S.T. (2002). Changes in expression of amyloid precursor protein and interleukin-1beta after experimental traumatic brain injury in rats. J Neurotrauma 19, 1555-1567.

97. Soininen, H., Solomon, A., Visser, P.J., Hendrix, S.B., Blennow, K., Kivipelto, M., Hartmann, T. and LipiDiDiet clinical study, g. (2017). 24-month intervention with a specific multinutrient in people with prodromal Alzheimer's disease (LipiDiDiet): a randomised, double-blind, controlled trial. Lancet Neurol 16, 965-975.

98. Povlishock, J.T. and Katz, D.I. (2005). Update of neuropathology and neurological recovery after traumatic brain injury. J Head Trauma Rehabil 20, 76-94.

99. Villapol, S., Yaszemski, A.K., Logan, T.T., Sanchez-Lemus, E., Saavedra, J.M. and Symes, A.J. (2012). Candesartan, an angiotensin II AT(1)-receptor blocker and PPAR-gamma agonist, reduces lesion volume and improves motor and memory function after traumatic brain injury in mice. Neuropsychopharmacology 37, 2817-2829.

100. Kumar, A. and Loane, D.J. (2012). Neuroinflammation after traumatic brain injury: opportunities for therapeutic intervention. Brain Behav Immun 26, 1191-1201.

101. Chen, M.K. and Guilarte, T.R. (2008). Translocator protein 18 kDa (TSPO): molecular sensor of brain injury and repair. Pharmacol Ther 118, 1-17.

102. Scott, G., Hellyer, P.J., Ramlackhansingh, A.F., Brooks, D.J., Matthews, P.M. and Sharp, D.J. (2015). Thalamic inflammation after brain trauma is associated with thalamo-cortical white matter damage. Journal of Neuroinflammation 12, 224.

103. Clarner, T., Diederichs, F., Berger, K., Denecke, B., Gan, L., van der Valk, P., Beyer, C., Amor, S. and Kipp, M. (2012). Myelin debris regulates inflammatory responses in an experimental demyelination animal model and multiple sclerosis lesions. Glia 60, 1468-1480.

104. Mannix, R.C. and Whalen, M.J. (2012). Traumatic brain injury, microglia, and Beta amyloid. Int J Alzheimers Dis 2012, 608732.

105. Suehiro, E. and Povlishock, J.T. (2001). Exacerbation of traumatically induced axonal injury by rapid posthypothermic rewarming and attenuation of axonal change by cyclosporin A. J Neurosurg 94, 493-498.

106. Smith, D.H., Chen, X.H., Iwata, A. and Graham, D.I. (2003). Amyloid [beta] accumulation in axons after traumatic brain injury in humans. J. Neurosurg. 98, 1072-1077.

107. Van Den Heuvel, C. (2007). Neurotrauma: New Insights into Pathology and Treatment Traumatic brain injury and Alzheimer's disease: a review. Progress in Brain Research 161, 303-316.

108. Johnson, V.E., Stewart, W. and Smith, D.H. (2010). Traumatic brain injury and amyloid-[beta] pathology: a link to Alzheimer's disease? Nat Rev Neurosci 11, 361-370.

109. Bush, T.G., Puvanachandra, N., Horner, C.H., Polito, A., Ostenfeld, T., Svendsen, C.N., Mucke, L., Johnson, M.H. and Sofroniew, M.V. (1999). Leukocyte infiltration, neuronal degeneration, and neurite outgrowth after ablation of scar-forming, reactive astrocytes in adult transgenic mice. Neuron 23, 297-308.

110. Tress, O., Maglione, M., May, D., Pivneva, T., Richter, N., Seyfarth, J., Binder, S., Zlomuzica, A., Seifert, G., Theis, M., Dere, E., Kettenmann, H. and Willecke, K. (2012). Panglial gap junctional communication is essential for maintenance of myelin in the CNS. J Neurosci 32, 7499-7518.

111. Shi, H., Hu, X., Leak, R.K., Shi, Y., An, C., Suenaga, J., Chen, J. and Gao, Y. (2015). Demyelination as a rational therapeutic target for ischemic or traumatic brain injury. Experimental Neurology 272, 17-25.

112. Richardson, R.M., Sun, D. and Bullock, M.R. (2007). Neurogenesis after traumatic brain injury. Neurosurg Clin N Am 18, 169-181, xi.

113. Xiong, Y., Mahmood, A. and Chopp, M. (2010). Angiogenesis, neurogenesis and brain recovery of function following injury. Curr Opin Investig Drugs 11, 298-308.

114. Xiong, Y., Mahmood, A., Zhang, Y., Meng, Y., Zhang, Z.G., Qu, C., Sager, T.N. and Chopp, M. (2011). Effects of posttraumatic carbamylated erythropoietin therapy on reducing lesion volume and hippocampal cell loss, enhancing angiogenesis and neurogenesis, and improving functional outcome in rats following traumatic brain injury. J Neurosurg 114, 549-559.

115. Han, X., Tong, J., Zhang, J., Farahvar, A., Wang, E., Yang, J., Samadani, U., Smith, D.H. and Huang, J.H. (2011). Imipramine treatment improves cognitive outcome associated with enhanced hippocampal neurogenesis after traumatic brain injury in mice. J Neurotrauma 28, 995-1007.

116. Nudo, R.J. (2013). Recovery after brain injury: mechanisms and principles. Front Hum Neurosci 7, 887.

117. Wang, K.C., Koprivica, V., Kim, J.A., Sivasankaran, R., Guo, Y., Neve, R.L. and He, Z. (2002). Oligodendrocyte-myelin glycoprotein is a Nogo receptor ligand that inhibits neurite outgrowth. Nature 417, 941-944.

118. Cansev, M., Watkins, C.J., van der Beek, E.M. and Wurtman, R.J. (2005). Oral uridine-5'-monophosphate (UMP) increases brain CDP-choline levels in gerbils. Brain Res 1058, 101-108.

119. de Wilde, M.C., Overk, C.R., Sijben, J.W. and Masliah, E. (2016). Meta-analysis of synaptic pathology in Alzheimer's disease reveals selective molecular vesicular machinery vulnerability. Alzheimers Dement 12, 633-644.

120. Emmerich, T., Abdullah, L., Ojo, J., Mouzon, B., Nguyen, T., Laco, G.S., Crynen, G., Evans, J.E., Reed, J., Mullan, M. and Crawford, F. (2017). Mild TBI Results in a Long-Term Decrease in Circulating Phospholipids in a Mouse Model of Injury. Neuromolecular Med 19, 122-135.

121. Stocchetti, N., Taccone, F.S., Citerio, G., Pepe, P.E., Le Roux, P.D., Oddo, M., Polderman, K.H., Stevens, R.D., Barsan, W., Maas, A.I., Meyfroidt, G., Bell, M.J., Silbergleit, R., Vespa, P.M., Faden, A.I., Helbok, R., Tisherman, S., Zanier, E.R., Valenzuela, T., Wendon, J., Menon, D.K. and Vincent, J.L. (2015). Neuroprotection in acute brain injury: an up-to-date review. Crit Care 19, 186.

122. Cansev, M., van Wijk, N., Turkyilmaz, M., Orhan, F., Sijben, J.W. and Broersen, L.M. (2015). Specific multi-nutrient enriched diet enhances hippocampal cholinergic transmission in aged rats. Neurobiol Aging 36, 344-351.

123. Olde Rikkert, M.G., Verhey, F.R., Blesa, R., von Arnim, C.A., Bongers, A., Harrison, J., Sijben, J., Scarpini, E., Vandewoude, M.F., Vellas, B., Witkamp, R., Kamphuis, P.J. and Scheltens, P. (2015). Tolerability and safety of Souvenaid in patients with mild Alzheimer's disease: results of multi-center, 24-week, open-label extension study. J Alzheimers Dis 44, 471-480.

124. de Waal, H., Stam, C.J., Lansbergen, M.M., Wieggers, R.L., Kamphuis, P.J., Scheltens, P., Maestu, F. and van Straaten, E.C. (2014). The effect of souvenaid on functional brain network organisation in patients with mild Alzheimer's disease: a randomised controlled study. PLoS One 9, e86558.

125. Loane, D.J. and Faden, A.I. (2010). Neuroprotection for traumatic brain injury: translational challenges and emerging therapeutic strategies. Trends Pharmacol Sci 31, 596-604.

126. Vonder Haar, C., Peterson, T.C., Martens, K.M. and Hoane, M.R. (2016). Vitamins and nutrients as primary treatments in experimental brain injury: Clinical implications for nutraceutical therapies. Brain Res 1640, Part A, 114-129.

127. Brown, C.E., Boyd, J.D. and Murphy, T.H. (2010). Longitudinal in vivo imaging reveals balanced and branch-specific remodeling of mature cortical pyramidal dendritic arbors after stroke. J Cereb Blood Flow Metab 30, 783-791.

128. Brown, C.E. and Murphy, T.H. (2008). Livin' on the Edge: Imaging Dendritic Spine Turnover in the Peri-Infarct Zone during Ischemic Stroke and Recovery. The Neuroscientist 14, 139-146.

129. Volz, L.J., Sarfeld, A.S., Diekhoff, S., Rehme, A.K., Pool, E.M., Eickhoff, S.B., Fink, G.R. and Grefkes, C. (2015). Motor cortex excitability and connectivity in chronic stroke: a multimodal model of functional reorganization. Brain Struct Funct 220, 1093-1107.

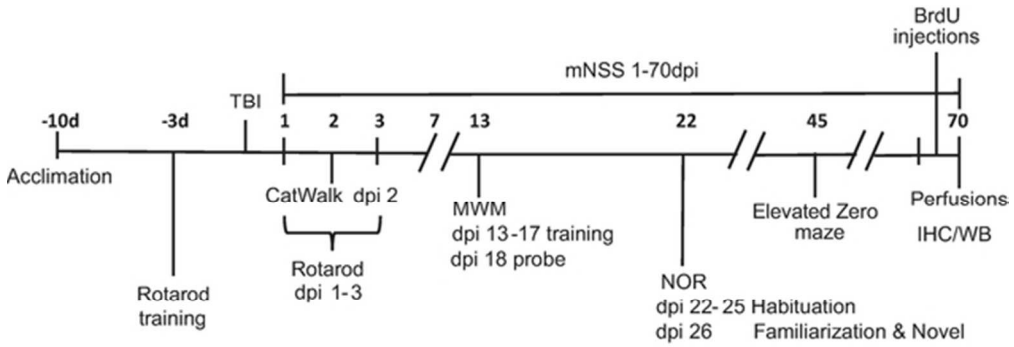

Experimental design. The behavioural testing was performed for 70 days post-injury (dpi). A controlled cortical impact (CCI) or a control craniotomy (sham injury) were induced in adult male mice. Animals were divided into 3 experimental groups (craniotomy-control, CCI-Control and CCI-FC). All mice were tested for motor and cognitive impairments on all behavioural tests. Mice were trained for three consecutive days for the Rotarod test prior to injury. Throughout the study (1-70 dpi), mice were tested for mNSS every other day on the first week and once a week thereafter, Rotarod (1-3 dpi), Catwalk (2 dpi), MWM (13-18 dpi), Novel Object Recognition (NOR) (22-26 dpi) and Elevated Zero Maze (EZM) (45 dpi). A week before the end of the study mice were injected twice a day with BrdU. Mice were monitored daily for weight and food consumption. On 70 dpi mice underwent perfusion for immunohistochemistry (IHC) analysis or were decapitated and brains were quickly removed and snap frozen for western blot (WB) analysis. 70d plasma and cerebellar tissue samples were used for lipid analysis.

53x20mm (300 x 300 DPI)

Table 1: Compositions of the experimental diets (g/100 g).

Ingredient	Control	FC
Corn starch	35,57	31,31
Caseine (>85% protein)	14,00	14,00
Corn dextrine	15,50	15,50
Sucrose	10,00	10,00
Dextrose	10,00	10,00
Fibre	5,00	5,00
Mineral mix (AIN-93M-MX)	3,50	3,50
Vitamin mix (AIN-93-VX)	1,00	1,00
Choline bitartrate (41,1% choline)	0,250	0,250
L-cystine	0,180	0,180
Tert-butylhydroquinone	0,0008	0,0008
Oil blends		
Soy oil	1,900	-
Coconut oil	0,900	0,100
Corn oil	2,200	0,100
DHA25 oil	-	4,500
EPA28/12	-	0,300
Other additions		
Pyridoxine-HCL	-	0,00529
Folic acid (90%)	-	0,00111
Cyanocobalamin (0,1% in mannitol)	-	0,00650
Ascorbic acid (100% pure)	-	0,24000
dl-α-tocopheryl acetate (500 IU/g)	-	0,70500
UMP disodium (24%H2O)	-	1,50000
Choline chloride (74,576 %)	-	0,67046
Soy lecithine (Emulpur)	-	1,13205
Total phospholipids	(-)	(0,8717)
Phosphatidylcholine	(-)	(0,2264)
Phosphatidylinositol	(-)	(0,1585)
Phosphatidylethanolamine	(-)	(0,1472)
Sodium selenite (46 % min)	-	0,00036
Total	100,0	100,0

Fatty acid profile	Control	FC
C-4:0	0,000	0,000
C-6:0	0,004	0,001
C-8:0	0,064	0,007
C-10:0	0,052	0,006
C-12:0	0,395	0,046
C-14:0	0,155	0,191
C-14:1 n5	0,000	0,000
C-15:0	0,000	0,035
C-16:0	0,492	0,795
C-16:1 n7	0,004	0,251
C-17:0	0,000	0,042
C-18:0	0,136	0,222
C-18:1 n9	1,041	0,656
C-18:2 n6	2,181	0,158
C-18:3 n3	0,107	0,038
C-18:3 n6	0,000	0,006
C-18:4 n3	0,000	0,001
C-20:0	0,020	0,018
C-20:1 n9	0,010	0,097
C-20:2 n6	0,000	0,035
C-20:3 n6	0,000	0,008
C-20:4 n3	0,000	0,000
C-20:4 n6	0,000	0,092
C-20:5 n3	0,000	0,433
C-22:0	0,009	0,011
C-22:1 n9	0,000	0,012
C-22:4 n6	0,000	0,017
C-22:5 n3	0,000	0,074
C-22:6 n3	0,000	1,117
C-24:0	0,000	0,008
C-24:1 n9	0,000	0,014
Total FA	4,771	4,771
SAT FA	1,327	1,382
MUFA	1,055	1,030
PUFA	2,288	1,979
Other FA	0,101	0,379
MCT	0,515	0,060
Tot n6	2,181	0,316
Tot n3	0,107	1,663
n6 / n3	20,298	0,190

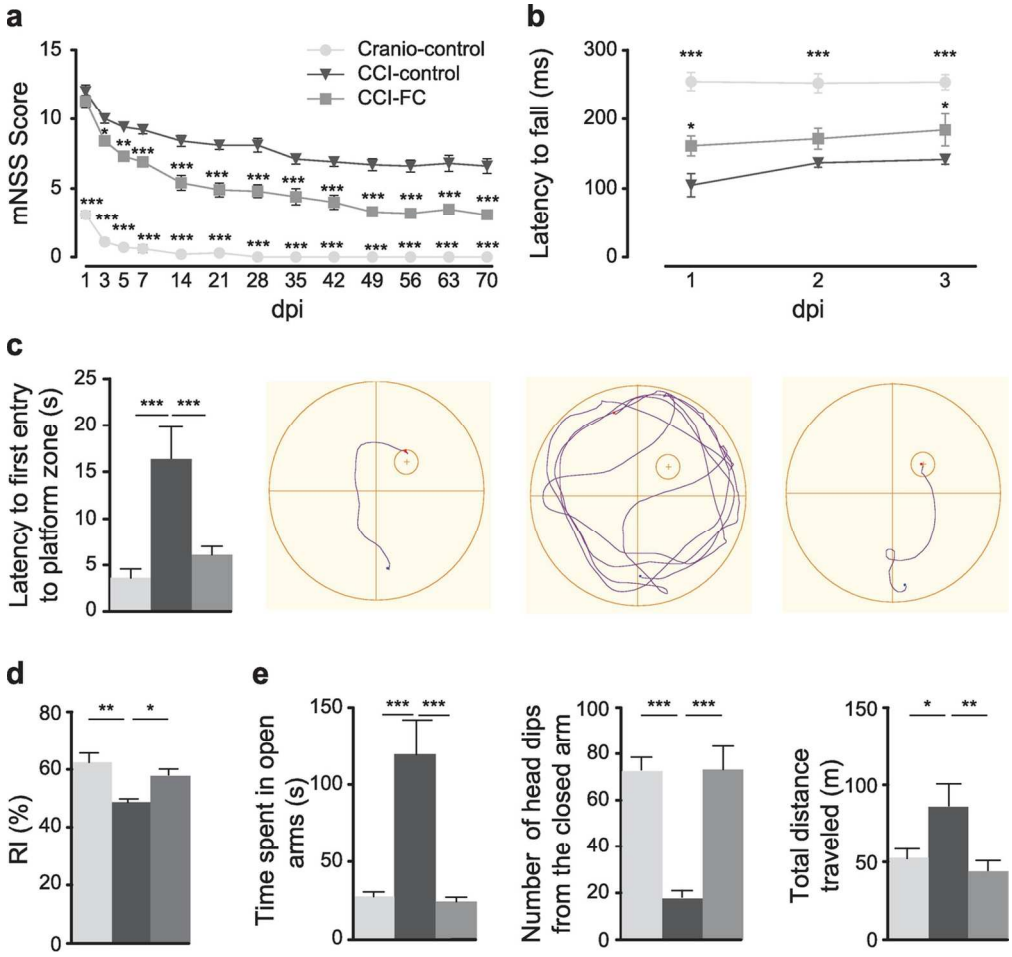

Integrated neurological function and motor assessments. mNSS (a) and Rotarod (b). (a). From 5 dpi and thereafter, the CCI-FC animals showed a significant improvement compared to the CCI-control group (Two way ANOVA; $p < 0.0001$, $F(2,27) = 320.8$; Bonferroni's post-hoc test **p<0.01***P<0.001); the craniotomy-control group showed significant improvement from 1 dpi and nearly no deficits after 14 dpi (***p<.001 compared to CCI-control). (b). On 1 and 3 dpi, CCI-FC and craniotomy-control mice showed marked improvement compared with the CCI-control mice (One way ANOVA; $p < 0.0001$, $F(2,26) = 42.31$; Bonferroni's post-hoc test *P<.05; ***P<.001, respectively). Data are means ± SEM of 10 animals/group. Cognitive performance assessments. MWM (c) and NOR (d). (c). A significant reduction in latency to the first entry to the platform-quadrant was seen in CCI-FC and craniotomy control animals in the probe test (One way ANOVA; $p = 0.0005$, $F(2,27) = 10.17$; Bonferroni's post-hoc test **P<0.01; ***P<0.001, respectively) compared with CCI-control animals. Underneath, an illustration of the track of an animal, from release into the water until it first entered the platform quadrant. (d). A significant increase in the time spent exploring a novel object, compared to the familiar one, was seen in both CCI-FC and craniotomy control mice compared to CCI-control mice (One way ANOVA; $p < 0.003$, $F(3,36) = 5.596$; Bonferroni's post-hoc test *P<0.05; **P<0.01, respectively). Results expressed as the Recognition Index (RI) %: the time spent investigating the novel object relative to the total time of object investigation. Data are means ± SEM of 10 animals per group.

Anxiety assessment. Elevated zero maze (EZM) (e). CCI-FC and craniotomy-control mice showed limited exploration of the unfamiliar environment, showed by (i) reduced preference for open zones, as reflected in total time spent in the open zone, (One way ANOVA; $p = 0.0004$, $F(2,12) = 16.52$; Bonferroni's post-hoc test ***P<0.001) compared with CCI-control animals. (ii). A lower number of head dips (One way ANOVA; $p = 0.0001$, $F(2,12) = 21.92$; Bonferroni's post-hoc test ***P<0.001) and (iii) A reduced total distance

travelled during the 5 min trial (One way ANOVA; p = 0.0068, F(2,12) = 7.799; Bonferroni's post-hoc test **p<0.01; *p <0.05, respectively). Data are means ± SEM of 10 animals/group.

122x115mm (300 x 300 DPI)

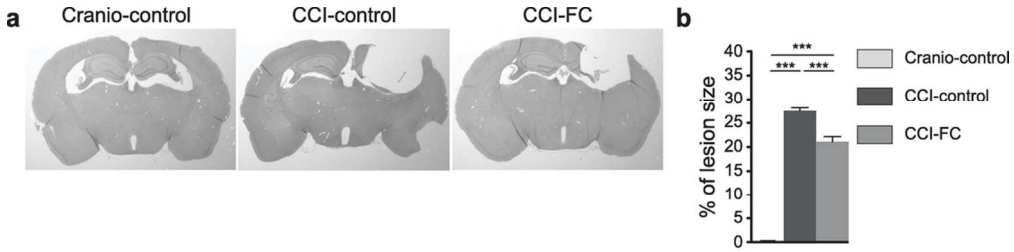

Lesion size (a,b). (a) Sections stained with H&E showing differences in lesion size. (b) Graph showing a significant reduction in lesion size in CCI-FC mice compared with CCI-control vs. craniotomy-control mice, at 70 days post-TBI (One way ANOVA; $p < 0.0001$, $F(2,33) = 382.5$; Bonferroni's post-hoc test; ***$p < 0.001$). Data are means ± SEM of 5 animals/group. Data are means ± SEM of 5 animals/group.

99x65mm (300 x 300 DPI)

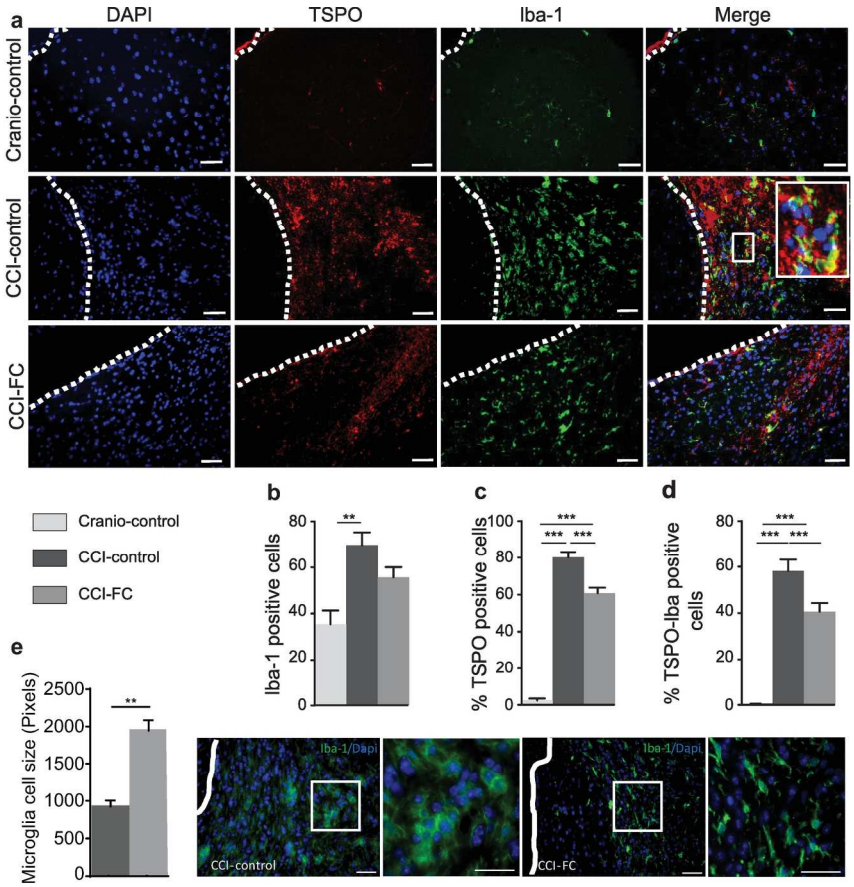

Neuroinflammatory response. (a) Images of DAPI, TSPO, Iba-1 and double-labelled TSPO/Iba-1 cells. Note the different microglia morphology (activation): amoeboid vs. ramified. Scale bars=100 µm. To show co-localization we enlarged the area marked with rectangle. Scale bars= 100 µm. Immunohistochemistry quantification, around the lesion border, of (b) %Iba-1 positive cells (One way ANOVA; p = 0.0032, F(2,11) = 10.1; Bonferroni's post-hoc test **p <0.01), (c) %TSPO positive cells (One way ANOVA; p < 0.0001, F(2,11) = 273.7; Bonferroni's post-hoc test *** p <0.001) and (d) Co-localised TSPO and Iba-1 positive cells (One way ANOVA; p < 0.0001, F(2,11) = 77.97; Bonferroni's post-hoc test ***p <0.001). (e) Microglia cell size analysis (Mann Whitney test **p= 0.0079) and corresponding images, showing the differences in cell size. The insets show the clear morphological differences. Scale bars= 100 µm. Data are means ± SEM of 5 animals/group.

183x226mm (300 x 300 DPI)

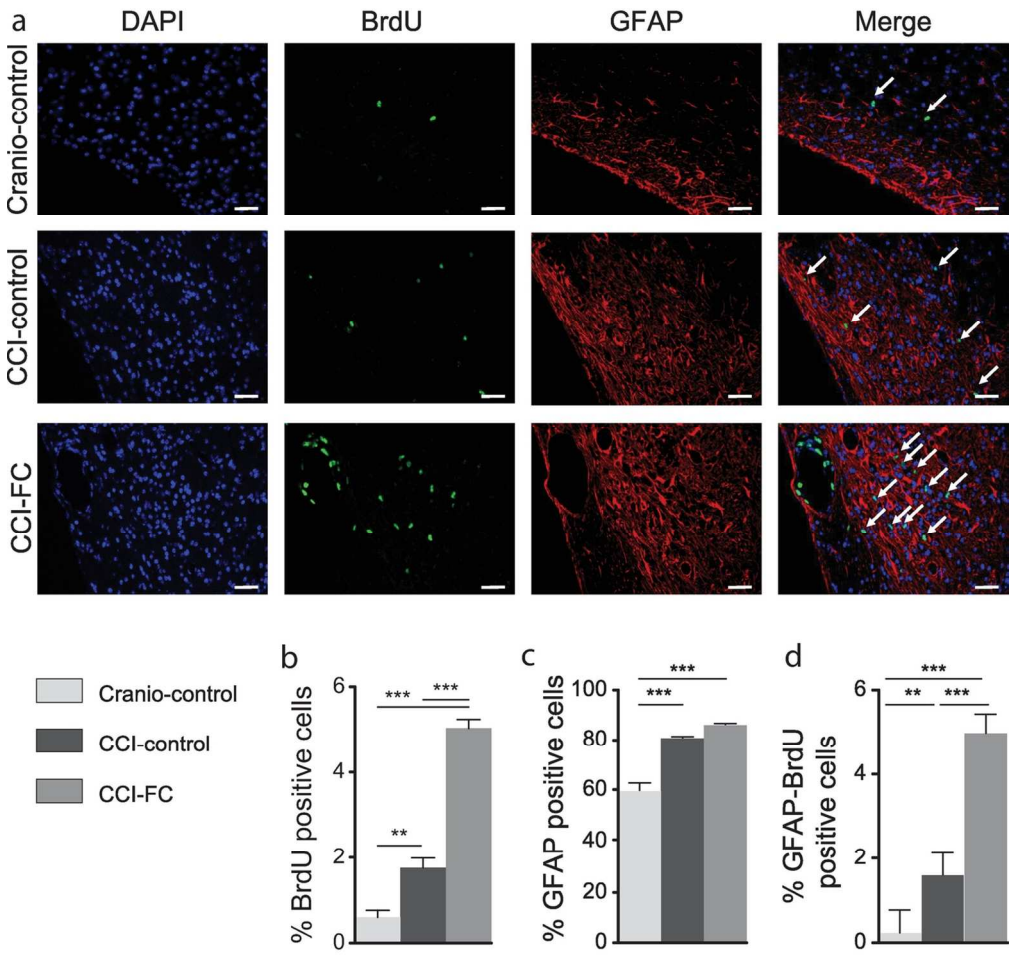

Astrocyte response post-injury. (a) Images of DAPI, BrdU, GFAP and double-labelled GFAP/BrdU cells. Arrows show co- localization. Scale bars=100 µm. Immunohistochemistry quantification, around the lesion border, of (b)% BrdU positive cells (One way ANOVA $p < 0.0001$, $F(2,12) = 131.5$; Bonferroni's post-hoc test **p<0.01***P<0.001). (c) %GFAP positive cells (One way ANOVA; $p < 0.0001$, $F(2,12) = 40.37$; Bonferroni's post-hoc test ***p <0.0001) and (d) Co-localised % GFAP and BrdU positive cells (One way ANOVA; $p < 0.0001$, $F(2,12) = 119.4$; Bonferroni's post-hoc test *** p <0.0001). Data are means ± SEM of 5 animals per group.

122x116mm (300 x 300 DPI)

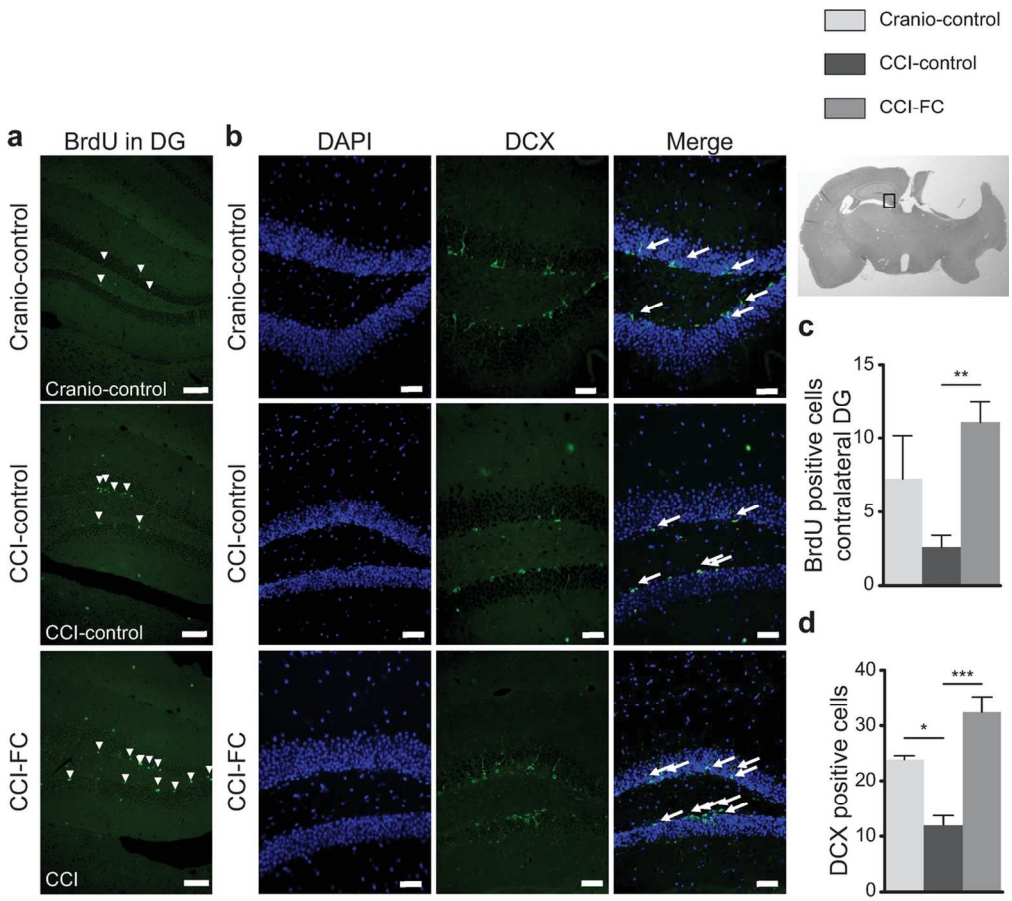

Cell proliferation and neurogenesis. (a) Images of BrdU in the contralateral DG. Scale bars=25μm. (c) Immunohistochemistry quantification of BrdU positive cells in the contralateral DG (One way ANOVA p = 0.0098, F(2,9) = 8.069; Bonferroni's post-hoc test **P<0.01). Data are means ± SEM of 5 animals/group. Number of positive DCX cells in the contralateral dentate gyrus (DG). (b) Images of DCX in the contralateral DG. Scale bars=25μm. (d) Quantification of DCX positive cells in the contralateral DG. (One way ANOVA p = 0.0009, F(2,6) = 27.64; Bonferroni's post-hoc test *P<0.05***P<0.001). Data are means ± SEM of 5 animals/group.

115x102mm (300 x 300 DPI)

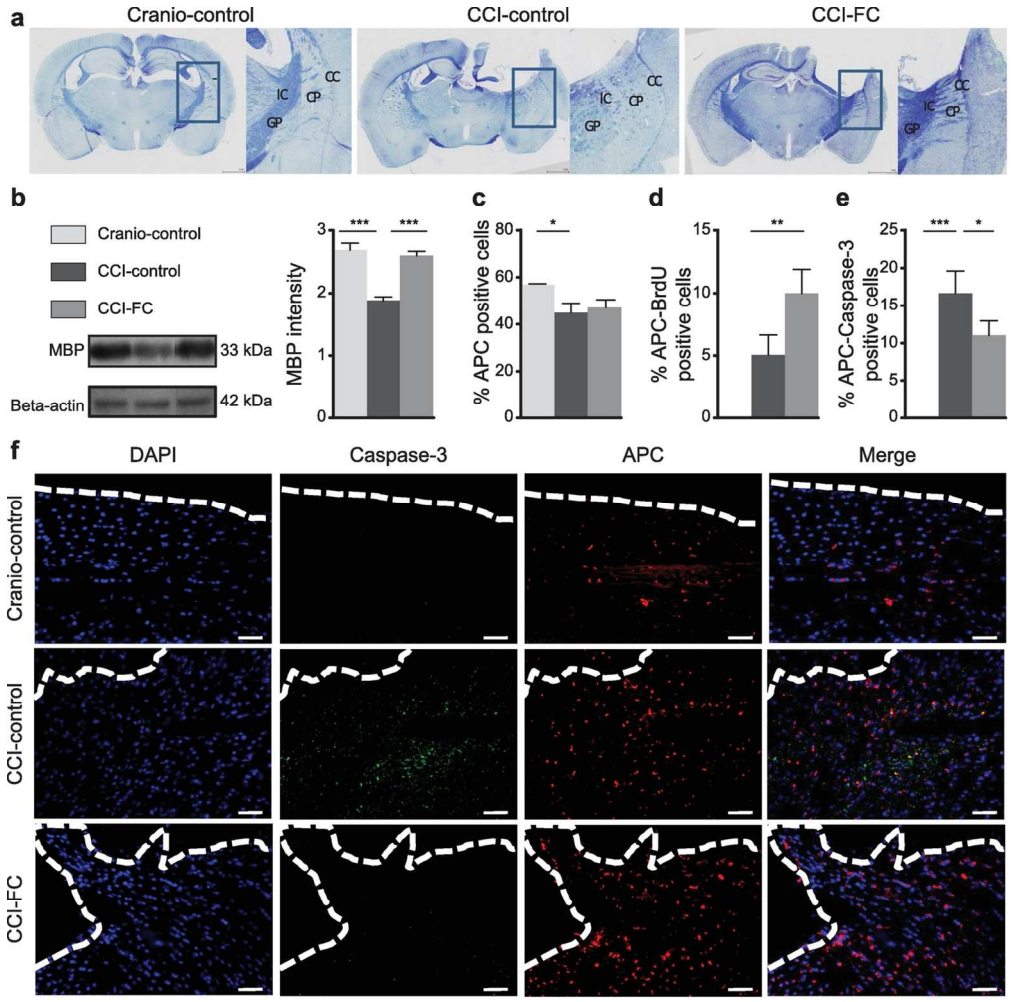

Myelin. (a) Coronal brain sections stained with Luxol Fast blue (LFB). Note differences in the internal capsule (IC), globus pallidus (GP)-external segment, caudate-putamen (CP) and corpus callosum (CC) regions (areas marked with rectangles and enlarged). In the CCI-FC and craniotomy control groups, myelin-stained tracts look continuous, in contrast with a doted pattern seen in the CCI-control group, both ipsilateral and contralateral to the injury site.

(b) Myelin Basic Protein levels (MBP) by Western blot. MBP 20kDa was significantly increased in the CCI-FC and craniotomy-control groups (One way ANOVA $p < 0.0001$, $F(2,12) = 27.81$; Bonferroni's post-hoc test ***$P<0.001$) compared with CCI-control mice.

Oligodendrocytes. (c) Quantification of oligodendrocytes (%APC positive cells) (One way ANOVA $p = 0.0417$, $F(2,9) = 4.619$; Bonferroni's post-hoc test *$p < 0.05$) (d) Dual staining APC and BrdU (One way ANOVA $p = 0.0028$, $F(2,9) = 12.09$; Bonferroni's post-hoc test **$P<0.01$). (e) Dual staining APC with caspase-3 (One way ANOVA $p = 0.0009$, $F(2,9) = 16.9$; Bonferroni's post-hoc test *$P<0.05$; ***$P<0.001$) and (f) Images of oligodendrocytes, caspase-3 and DAPI around the lesion border. Scale bar=100 µm. Data are means ± SEM of 5 animals/group.

127x126mm (300 x 300 DPI)

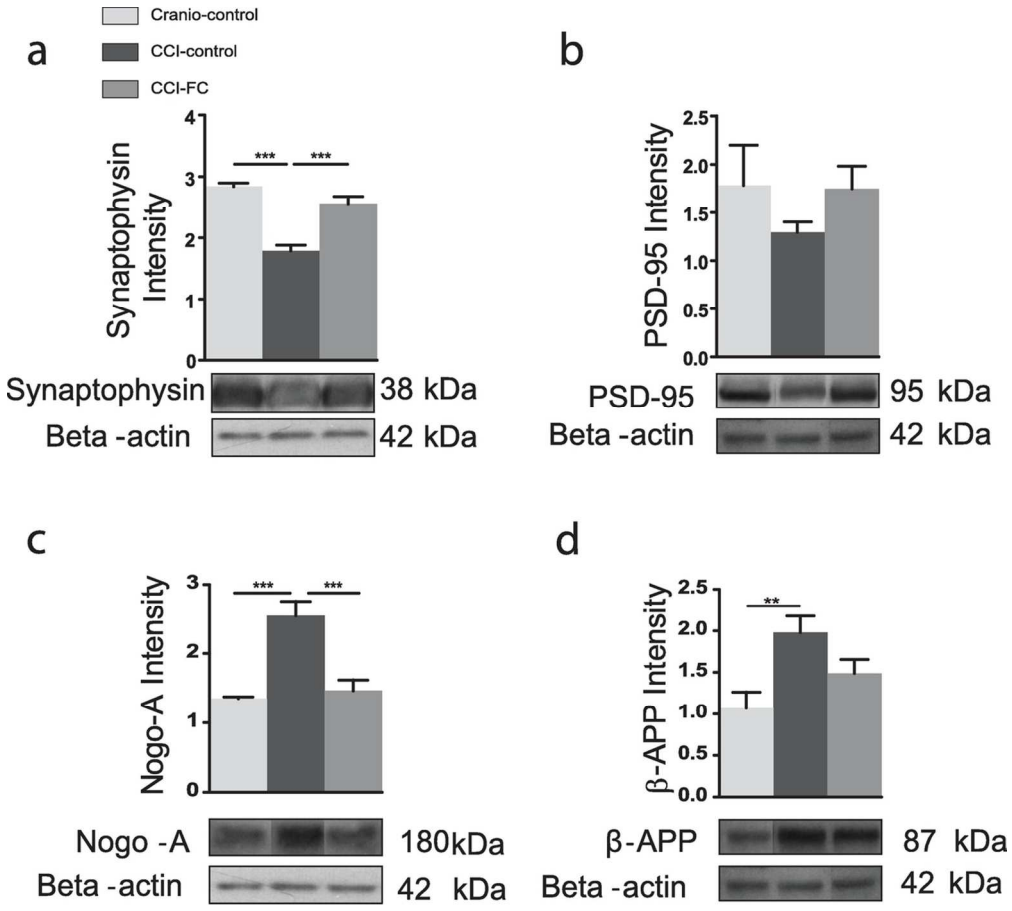

Synaptic markers. Graph and cropped gels of WB analysis of protein levels of (a) Synaptophysin; 38kDa (One way ANOVA $p < 0.0001$, $F(2,12) = 35.5$; Bonferroni's post-hoc test ***P<0.001) and (b) PSD-95; 95kDa (One way ANOVA $p = 0.4188$, $F(2,12) = 0.9365$; Bonferroni's post-hoc test #P<0.06) were analyzed by Western blot. Data are means ± SEM of 5 animals/group.
Neurite outgrowth inhibitor and amyloid load. (c) Graph and cropped gels of WB analysis of protein levels of Nogo-A; 180kD (One way ANOVA $p = 0.0002$, $F(2,12) = 18.68$; Bonferroni's post-hoc test ***P<0.001) and (d) β-APP; 87 kDa (One way ANOVA $p = 0.0163$, $F(2,12) = 5.915$; Bonferroni's post-hoc test **P<0.01) were analysed in both the CCI-FC and craniotomy control mice compared with CCI-control mice. Data are mean ± SEM of 5 animals/group. β-actin was used as loading control.

112x101mm (300 x 300 DPI)

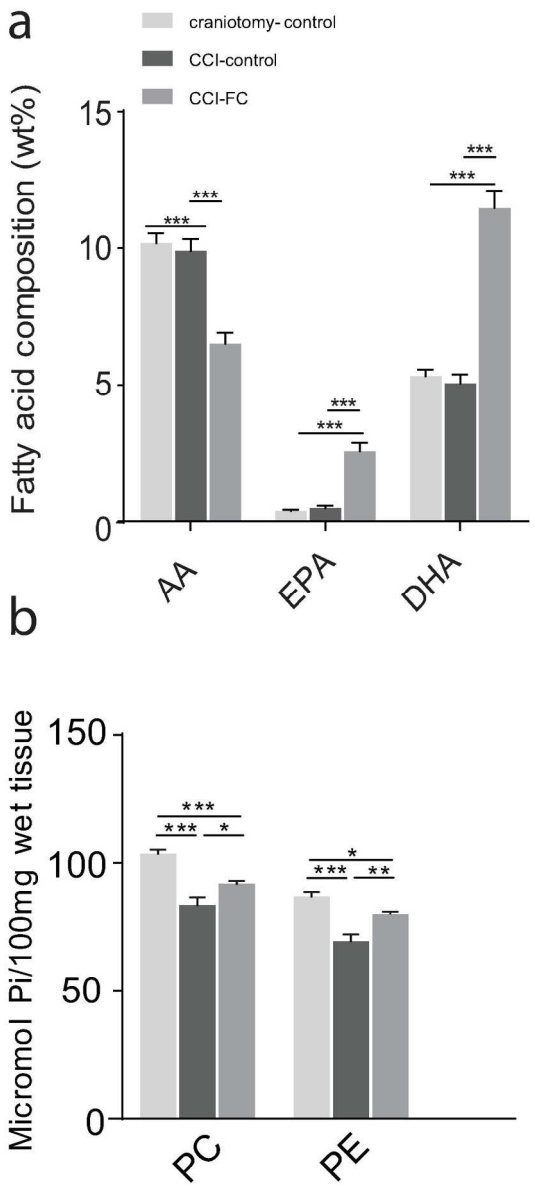

Phospholipid fatty acid composition in plasma and the tissue phospholipids. In plasma (a) a significant reduction in AA and increases in EPA and DHA in CCI-FC mice compared with CCI-control and craniotomy-control at 70 days post-TBI (One way ANOVA p <0.0001, F(2,93) = 20.45; Bonferroni's post-hoc test ***p <0.001). Data are means ± SEM of 5 animals/group. In cerebellum (b) a reduction in tissue PC levels by 20% in injured animals on the control diet vs. craniotomy controls, reduced to 11% in the FC supplementation group compared with craniotomy controls. (One way ANOVA p <0.0001, F(2, 3) = 26.99; Bonferroni's post-hoc test ***p <0.001). Data are means ± SEM of 5 animals/group. PE levels decreased by 21% in the injured animals on the control diet vs. craniotomy-only, while after FC supplementation the difference vs. craniotomy controls was only 8%.(One way ANOVA p <0.0001, F(2, 3) = 20.82; Bonferroni's post-hoc test ***p <0.001). Data are means ± SEM of 5 animals/group.

123x283mm (300 x 300 DPI)

Figure 1.

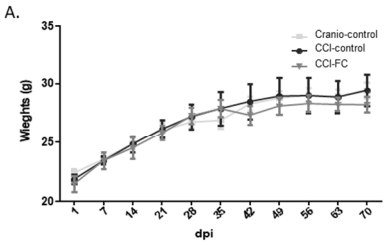

Body weight comparison among all experimental groups. Graph showing weekly measurement of average group weights with no differences between diets. Data are means ± SEM of 10 animals/group.

338x297mm (96 x 96 DPI)

Figure 2.

Task	Score
Exit-time*	1-3
Walking straight	1
Startle reflex	1
Seeking behaviour	1
Hemiparesis	1
Round stick balance	1
Triangle stick balance	1
Beam walking**	
1cm	1-3
2cm	1-3
3cm	1-3

*Exit task-points	Score
exit within 20sec	0
exit within 60sec	1
exit within 2min	2
no exit within 2min	3
**Beam walk-points	
Balance and walk with normal posture	0
Grasp side of the beam+ draging OR sliping poterior paw less than 3 times	1
more than 3 times and no abiliti togrip	2
unable to walk the beam	3

Modified neurological severity score test (mNSS)-table of content Modified Neurological severity scores (NSS) outlined in Table. This modified test consists of 10 individual clinical parameters, including tasks on motor function, alertness and physiological behaviour, to evaluate the neurological impairment. One point is awarded for the inability to perform the tasks. A maximal NSS of 18 points thus indicates severe neurological dysfunction, with failure of all tasks. Modifications of the scoring are represented with asterisks and detailed respectively in the second table.

338x297mm (96 x 96 DPI)

Figure 3.

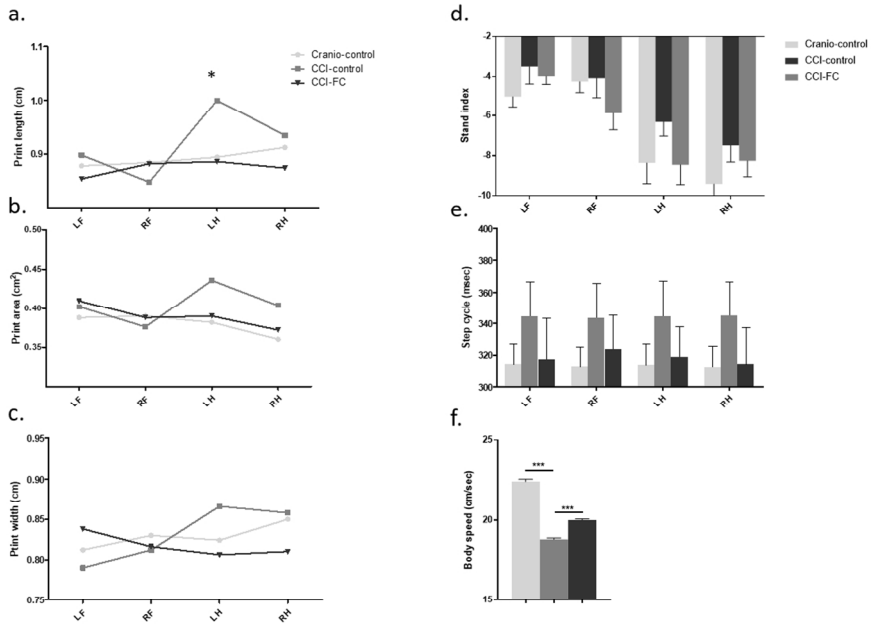

Gait impairment assessment after TBI was assessed at 2dpi, using the CatWalk XT system. Behaviour data was analysed using two-way ANOVA analysis. The FC-treated group showed a decrease in (a) print length (horizontal direction; LH *p< 0.05 compared to CCI-control) on the side contralateral to the injury, with an emphasis on the left hind paw. A longer print length could reflect foot dragging and overall less control of the foot. We also noticed a clear tendency to a smaller(b) print width and (c) print area (vertical direction) in the CCI-control group (ns, Two-way ANOVA**p<0.01). The Stand Index (SI) was higher in CCI-control animals compared with the two other groups (***p<0.001; d) The overall step cycle (e) was longer and the body speed (f), significantly slower in the CCI-control group compared to CCI-FC and craniotomy-control (ns, Two-way ANOVA *p< 0.05 subjects, Bonferroni post-hoc test: ***p<0.0001 respectively. Data are means ± SEM of 10 animals/group.

338x297mm (96 x 96 DPI)

Figure 4.

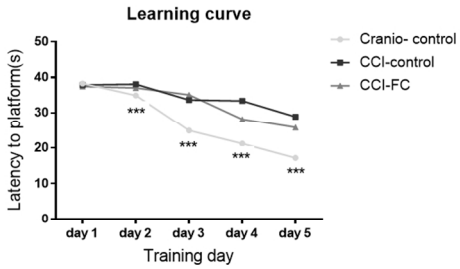

Evaluation of learning acquisition curve in MWM test Five consecutive days of acquisition training sessions were assessed on 13-17dpi. The mean latencies to find the platform was recorded. Two-way ANOVA ***p< 0.001, Bonferroni post-hoc test: Day2- Cranio- control vs. CCI-control and CCI-FC ***p<0.001; Day3- Cranio- control vs. CCI-control and CCI-FC ***p<0.001; Day4- all group comparison ***p<0.001; Day5- Cranio- control vs. CCI-control ***p<0.001 and Cranio- control vs. CCI-FC *p<0.05). Data are means ± SEM of 10 animals/group.

338x297mm (96 x 96 DPI)

Figure 5.

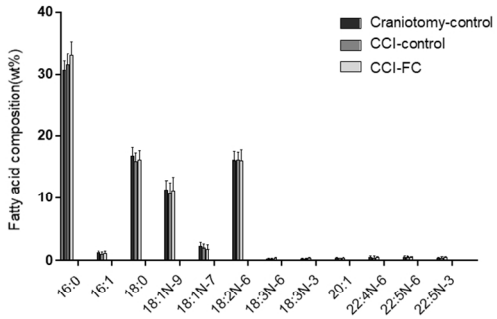

Other fatty acid composition. The total phospholipid fatty acid content of the plasma samples was determined. Data are means ± SEM of 10 animals/group.

338x297mm (96 x 96 DPI)

Figure legends

Fig. 1

Experimental design. The behavioural testing was performed for 70 days post-injury (dpi). A controlled cortical impact (CCI) or a control craniotomy (sham injury) were induced in adult male mice. Animals were divided into 3 experimental groups (craniotomy-control, CCI-Control and CCI-FC). All mice were tested for motor and cognitive impairments on all behavioural tests. Mice were trained for three consecutive days for the Rotarod test prior to injury. Throughout the study (1-70 dpi), mice were tested for mNSS every other day on the first week and once a week thereafter, Rotarod (1-3 dpi), Catwalk (2 dpi), MWM (13-18 dpi), Novel Object Recognition (NOR) (22-26 dpi) and Elevated Zero Maze (EZM) (45 dpi). A week before the end of the study mice were injected twice a day with BrdU. Mice were monitored daily for weight and food consumption. On 70 dpi mice underwent perfusion for immunohistochemistry (IHC) analysis or were decapitated and brains were quickly removed and snap frozen for western blot (WB) analysis. 70d plasma and cerebellar tissue samples were used for lipid analysis.

Table 1

Composition of the experimental diets (g/100 g).

Fig. 2

Integrated neurological function and motor assessments. mNSS (a) and Rotarod (b). (a). From 5 dpi and thereafter, the CCI-FC animals showed a significant improvement compared to the CCI-control group (Two way ANOVA; $p < 0.0001$, $F_{(2,27)} = 320.8$; Bonferroni's post-hoc test **p<0.01***P<0.001); the craniotomy-control group showed significant improvement from 1 dpi and nearly no deficits after 14 dpi (***p<.001 compared to CCI-control). (b). On 1 and 3 dpi, CCI-FC and craniotomy-control mice showed marked improvement compared with the CCI-

control mice (One way ANOVA; $p < 0.0001$, $F_{(2,26)} = 42.31$; Bonferroni's post-hoc test *P<.05; ***P<.001, respectively). Data are means ± SEM of 10 animals/group.

Cognitive performance assessments. MWM (c) and NOR (d). (c). A significant reduction in latency to the first entry to the platform-quadrant was seen in CCI-FC and craniotomy control animals in the probe test (One way ANOVA; $p = 0.0005$, $F_{(2,27)} = 10.17$; Bonferroni's post-hoc test **P<0.01; ***P<0.001, respectively) compared with CCI-control animals. Underneath, an illustration of the track of an animal, from release into the water until it first entered the platform quadrant. (d). A significant increase in the time spent exploring a novel object, compared to the familiar one, was seen in both CCI-FC and craniotomy control mice compared to CCI-control mice (One way ANOVA; $p < 0.003$, $F_{(3,36)} = 5.596$; Bonferroni's post-hoc test *P<0.05; **P<0.01, respectively). Results expressed as the Recognition Index (RI) %: the time spent investigating the novel object relative to the total time of object investigation. Data are means ± SEM of 10 animals per group.

Anxiety assessment. Elevated zero maze (EZM) (e). CCI-FC and craniotomy-control mice showed limited exploration of the unfamiliar environment, showed by (i) reduced preference for open zones, as reflected in total time spent in the open zone, (One way ANOVA; $p = 0.0004$, $F_{(2,12)} = 16.52$; Bonferroni's post-hoc test ***P<0.001) compared with CCI-control animals. (ii). A lower number of head dips (One way ANOVA; $p = 0.0001$, $F_{(2,12)} = 21.92$; Bonferroni's post-hoc test ***P<0.001) and (iii) A reduced total distance travelled during the 5 min trial (One way ANOVA; $p = 0.0068$, $F_{(2,12)} = 7.799$; Bonferroni's post-hoc test **p<0.01; *p <0.05, respectively). Data are means ± SEM of 10 animals/group.

Fig 3.

Lesion size (a,b). (a) Sections stained with H&E showing differences in lesion size. (b) Graph showing a significant reduction in lesion size in CCI-FC mice compared with CCI-control vs.

craniotomy-control mice, at 70 days post-TBI (One way ANOVA; $p < 0.0001$, $F_{(2,33)} = 382.5$; Bonferroni's post-hoc test; ***p <0.001). Data are means ± SEM of 5 animals/group. Data are means ± SEM of 5 animals/group.

Fig 4.

Neuroinflammatory response. (a) Images of DAPI, TSPO, Iba-1 and double-labelled TSPO/Iba-1 cells. Note the different microglia morphology (activation): amoeboid vs. ramified. Scale bars=100 µm. To show co-localization we enlarged the area marked with rectangle. Scale bars= 100 µm. Immunohistochemistry quantification, around the lesion border, of (b) %Iba-1 positive cells (One way ANOVA; $p = 0.0032$, $F_{(2,11)} = 10.1$; Bonferroni's post-hoc test **p <0.01), (c) %TSPO positive cells (One way ANOVA; $p < 0.0001$, $F_{(2,11)} = 273.7$; Bonferroni's post-hoc test *** p <0.001) and (d) Co-localised TSPO and Iba-1 positive cells (One way ANOVA; $p < 0.0001$, $F_{(2,11)} = 77.97$; Bonferroni's post-hoc test ***p <0.001). (e) Microglia cell size analysis (Mann Whitney test **p= 0.0079) and corresponding images, showing the differences in cell size. The insets show the clear morphological differences. Scale bars= 100 µm. Data are means ± SEM of 5 animals/group.

Fig 5.

Astrocyte response post-injury. (a) Images of DAPI, BrdU, GFAP and double-labelled GFAP/BrdU cells. Arrows show co- localization. Scale bars=100 µm. Immunohistochemistry quantification, around the lesion border, of (b)% BrdU positive cells (One way ANOVA $p < 0.0001$, $F_{(2,12)} = 131.5$; Bonferroni's post-hoc test **p<0.01***P<0.001). (c) %GFAP positive cells (One way ANOVA; $p < 0.0001$, $F_{(2,12)} = 40.37$; Bonferroni's post-hoc test ***p <0.0001) and (d) Co-localised % GFAP and BrdU positive cells (One way ANOVA; $p < 0.0001$, $F_{(2,12)} = 119.4$; Bonferroni's post-hoc test *** p <0.0001). Data are means ± SEM of 5 animals per group.

Fig 6.

Cell proliferation and neurogenesis. (a) Images of BrdU in the contralateral DG. Scale bars=25µm. (c) Immunohistochemistry quantification of BrdU positive cells in the contralateral DG (One way ANOVA $p = 0.0098$, $F_{(2,9)} = 8.069$; Bonferroni's post-hoc test **P<0.01). Data are means ± SEM of 5 animals/group.

Number of positive DCX cells in the contralateral dentate gyrus (DG). (b) Images of DCX in the contralateral DG. Scale bars=25µm. (d) Quantification of DCX positive cells in the contralateral DG. (One way ANOVA $p = 0.0009$, $F_{(2,6)} = 27.64$; Bonferroni's post-hoc test *P<0.05***P<0.001). Data are means ± SEM of 5 animals/group.

Fig 7.

Myelin. (a) Coronal brain sections stained with Luxol Fast blue (LFB). Note differences in the internal capsule (IC), globus pallidus (GP)-external segment, caudate-putamen (CP) and corpus callosum (CC) regions (areas marked with rectangles and enlarged). In the CCI-FC and craniotomy control groups, myelin-stained tracts look continuous, in contrast with a doted pattern seen in the CCI-control group, both ipsilateral and contralateral to the injury site.

(b) Myelin Basic Protein levels (MBP) by Western blot. MBP 20kDa was significantly increased in the CCI-FC and craniotomy-control groups (One way ANOVA p <0.0001, $F_{(2,12)} = 27.81$; Bonferroni's post-hoc test ***P<0.001) compared with CCI-control mice.

Oligodendrocytes. (c) Quantification of oligodendrocytes (%APC positive cells) (One way ANOVA $p = 0.0417$, $F_{(2,9)} = 4.619$; Bonferroni's post-hoc test *p <0.05) (d) Dual staining APC and BrdU (One way ANOVA $p = 0.0028$, $F_{(2,9)} = 12.09$; Bonferroni's post-hoc test **P<0.01). (e) Dual staining APC with caspase-3 (One way ANOVA $p = 0.0009$, $F_{(2,9)} = 16.9$; Bonferroni's post-hoc test *P<0.05; ***P<0.001) and (f) Images of oligodendrocytes, caspase-3 and DAPI around the lesion border. Scale bar=100 µm. Data are means ± SEM of 5 animals/group.

Fig 8.

Synaptic markers. Graph and cropped gels of WB analysis of protein levels of (a) Synaptophysin; 38kDa (One way ANOVA $p < 0.0001$, $F_{(2,12)} = 35.5$; Bonferroni's post-hoc test ***P<0.001) and (b) PSD-95; 95kDa (One way ANOVA $p = 0.4188$, $F_{(2,12)} = 0.9365$; Bonferroni's post-hoc test #P<0.06) were analyzed by Western blot. Data are means ± SEM of 5 animals/group.

Neurite outgrowth inhibitor and amyloid load. (c) Graph and cropped gels of WB analysis of protein levels of Nogo-A; 180kD (One way ANOVA $p = 0.0002$, $F_{(2,12)} = 18.68$; Bonferroni's post-hoc test ***P<0.001) and (d) β-APP; 87 kDa (One way ANOVA $p = 0.0163$, $F_{(2,12)} = 5.915$; Bonferroni's post-hoc test **P<0.01) were analysed in both the CCI-FC and craniotomy control mice compared with CCI-control mice. Data are mean ± SEM of 5 animals/group. β-actin was used as loading control.

Fig 9.

Phospholipid fatty acid composition in plasma and the tissue phospholipids. In plasma (a) a significant reduction in AA and increases in EPA and DHA in CCI-FC mice compared with CCI-control and craniotomy-control at 70 days post-TBI (One way ANOVA p <0.0001, $F_{(2,93)} = 20.45$; Bonferroni's post-hoc test ***p <0.001). Data are means ± SEM of 5 animals/group. In cerebellum (b) a reduction in tissue PC levels by 20% in injured animals on the control diet vs. craniotomy controls, reduced to 11% in the FC supplementation group compared with craniotomy controls. (One way ANOVA p <0.0001, $F_{(2, 3)} = 26.99$; Bonferroni's post-hoc test ***p <0.001). Data are means ± SEM of 5 animals/group. PE levels decreased by 21% in the injured animals on the control diet vs. craniotomy-only, while after FC supplementation the difference vs. craniotomy controls was only 8%.(One way ANOVA p <0.0001, $F_{(2, 3)} = 20.82$; Bonferroni's post-hoc test ***p <0.001). Data are means ± SEM of 5 animals/group.

Supplementary legends

Figure 1. Body weight comparison among all experimental groups. Graph showing weekly measurement of average group weights with no differences between diets. Data are means ± SEM of 10 animals/group.

Figure 2. Modified neurological severity score test (mNSS)-table of content Modified Neurological severity scores (NSS) outlined in Table. This modified test consists of 10 individual clinical parameters, including tasks on motor function, alertness and physiological behaviour, to evaluate the neurological impairment. One point is awarded for the inability to perform the tasks. A maximal NSS of 18 points thus indicates severe neurological dysfunction, with failure of all tasks. Modifications of the scoring are represented with asterisks and detailed respectively in the second table.

Figure 3. Gait impairment assessment after TBI was assessed at 2dpi, using the CatWalk XT system. Behaviour data was analysed using two-way ANOVA analysis. The FC-treated group showed a decrease in (a) print length (horizontal direction; LH *p< 0.05 compared to CCI-control) on the side contralateral to the injury, with an emphasis on the left hind paw. A longer print length could reflect foot dragging and overall less control of the foot. We also noticed a clear tendency to a smaller(b) print width and (c) print area (vertical direction) in the CCI-control group (ns, Two-way ANOVA**p<0.01). The Stand Index (SI) was higher in CCI-control animals compared with the two other groups (***p<0.001; d) The overall step cycle (e) was longer and the body speed (f), significantly slower in the CCI-control group compared to CCI-FC and craniotomy-control (ns, Two-way ANOVA *p< 0.05 subjects, Bonferroni post-hoc test: ***p<0.0001 respectively. Data are means ± SEM of 10 animals/group.

Figure 4. Evaluation of learning acquisition curve in MWM test Five consecutive days of acquisition training sessions were assessed on 13-17dpi. The mean latencies to find the platform was recorded. Two-way ANOVA ***p< 0.001, Bonferroni post-hoc test: Day2- Cranio- control vs. CCI-control and CCI-FC ***p<0.001; Day3- Cranio- control vs. CCI-control and CCI-FC ***p<0.001; Day4- all group comparison ***p<0.001; Day5- Cranio- control vs. CCI-control ***p<0.001 and Cranio- control vs. CCI-FC *p<0.05). Data are means ± SEM of 10 animals/group.

Figure 5. Other fatty acid composition. The total phospholipid fatty acid content of the plasma samples was determined. Data are means ± SEM of 10 animals/group.